Available online at www.sciencedirect.com

ScienceDirect

Nuclear Physics B 897 (2015) 346–373

NUCLEAR PHYSICS B

www.elsevier.com/locate/nuclphysb

On factorization of multiparticle pentagons

A.V. Belitsky

Department of Physics, Arizona State University, Tempe, AZ 85287-1504, USA

Received 9 March 2015; received in revised form 29 April 2015; accepted 21 May 2015

Available online 3 June 2015

Editor: Stephan Stieberger

Abstract

We address the near-collinear expansion of multiparticle NMHV amplitudes, namely, the heptagon and octagons in the dual language of null polygonal super Wilson loops. In particular, we verify multiparticle factorization of charged pentagon transitions in terms of pentagons for single flux-tube excitations within the framework of refined operator product expansion. We find a perfect agreement with available tree and one-loop data.

1. Introduction

The theory of the color flux-tube in planar maximally supersymmetric gauge theory is deeply rooted in the integrability of the model [1]. Recently an operator product expansion (OPE) in terms of its fundamental excitations was successfully formulated [2,3] to compute the expectation value of null polygonal supersymmetric Wilson loop $\mathcal{W}$ to any order of 't Hooft coupling. The superloop is dual to the on-shell scattering superamplitude [4–9] and thus promises one to provide nonperturbatively the complete S-matrix of the super Yang–Mills theory in question. Since the latter is a superconformal theory and thus does not possess asymptotic particle states in four-dimensions, one has to deal with regularized and properly subtracted combinations of amplitudes, known as ratio functions [10,11]. The refined version of the operator product expansion approach employs the so-called pentagon transitions $P(\psi|\psi')$ between eigenstates ψ and ψ' of the color flux tube [3]. An eigenstate ψ is parametrized by the eigenvalues of three generators

E-mail address: andrei.belitsky@asu.edu.

http://dx.doi.org/10.1016/j.nuclphysb.2015.05.024

of the conformal group which yield the energy E_ψ, momentum p_ψ and helicity m_ψ of the state. The dispersion relation $E = E(p)$ for the latter is conveniently parametrized by the excitation's rapidity u, such that $E = E(u)$ and $p = p(u)$. The latter are known to all orders in 't Hooft coupling for any excitations propagating on the flux tube [12].

An N-sided super Wilson loop $\mathcal{W}_N$ in a chosen tessellation is then decomposed in terms of pentagons as shown in Fig. 1 and reads [3]

$$\mathcal{W}_N = \int d\mu_\psi(\boldsymbol{u}) F_\psi(0|\boldsymbol{u}) P_{\bar\psi|\psi'}(-\bar{\boldsymbol{u}}|\boldsymbol{v}) d\mu_{\psi'}(\boldsymbol{v}) P_{\bar\psi'|\psi''}(-\bar{\boldsymbol{v}}|\boldsymbol{w}) \dots . \tag{1}$$

For this polygon, there are $N-6$ intermediate pentagons P, which together with the first and last ones, — dubbed creation/absorption form factors F for incoming/outgoing states, — overlap on $N-5$ intermediate squares. The latter are encoded in the measures $d\mu$ that cumulatively depend on $3(N-5)$ independent conformal cross ratios τ_j, σ_j and ϕ_j. For a given intermediate transition, $d\mu$ gets contribution from an n-particle state which admits a factorized form

$$d\mu_\psi(\boldsymbol{u}) \equiv \prod_{j=1}^{n} d\mu_{\mathrm{p}_j}(u_j)\,, \qquad d\mu_{\mathrm{p}_j}(u_j) = \frac{du_j}{2\pi}\,\mu_{\mathrm{p}_j}(u_j)\,\mathrm{e}^{-\tau E_{\mathrm{p}_j}(u_j)+i\sigma p_{\mathrm{p}_j}(u_j)+i\phi m_{\mathrm{p}_j}}\,. \tag{2}$$

Here and below, we will associate the first set of the cross ratios τ_1, σ_1, ϕ_1 with excitation rapidities $\boldsymbol{u}$, the second set τ_2, σ_2, ϕ_2 with $\boldsymbol{v}$, τ_3, σ_3, ϕ_3 with $\boldsymbol{w}$ etc. Above, the first and last pentagon transitions differ from all intermediate ones by the fact that their initial and final states, respectively, correspond to the flux-tube vacuum, however they are related to the rest by mirror transformations [3,13]. The chosen conventions were adopted from the integrability-based pentagon framework which one uses to compute all ingredients to any order of perturbation theory [3,14–19] from a set of axioms [3]. Hence, we employed the following notations in Eq. (1): while ψ corresponds to a collection of excitations in particular order $\psi = \{\mathrm{p}_1, \dots, \mathrm{p}_n\}$, $\bar\psi$ stands for its opposite $\bar\psi = \{\mathrm{p}_n, \dots, \mathrm{p}_1\}$. The same nomenclature applies to their rapidities associated with the corresponding flux-tube excitations, $\boldsymbol{u} = \{u_1, \dots, u_n\}$ and $\bar{\boldsymbol{u}} = \{u_n, \dots, u_1\}$, respectively.

The integrals over the rapidities of the flux-tube excitations in the formula (1) go over specific contours. The latter are the same for both holes and gauge fields which run along the real axis (or slightly above it in the complex plane). The most complicated contour C is the one for fermionic excitations [15]. It travels over a two-sheeted Riemann surface with a cut along the interval on the real axis $[-2g, 2g]$: in a nutshell, it is conveniently decomposed within perturbation theory into two contours $C = C_{\mathrm{F}} \cup C_{\mathrm{f}}$, with C_{F} that lies on the so-called large fermion sheet and runs just above the real axis, $C_{\mathrm{F}} = (-\infty + i0, +\infty + i0)$, the second one is a half-circle closed contour C_{f} on the small fermion sheet in the lower half plane of the complex rapidity plane. Having spelled out these explicitly, in what follows, we will not display the integration domains explicitly.

The OPE for the hexagon was addressed in great detail in previous studies [3,14–18] and successfully compared with available higher-loop data on scattering amplitudes[1] [20–25]. In this paper, we will address the question of computing higher-point null polygons[2] within the OPE framework paying special attention to the factorizability of multiparticle pentagons in terms of single particle ones. For identical excitations, its form was conjectured in Ref. [3] to be

[1] Quite recently similar results were obtained for the symbol of MHV heptagon in Refs. [26–29] up to three loop order.

[2] I would like to thank Benjamin Basso for informing me about analogous analysis currently under way [30] following the formalism of Ref. [19].

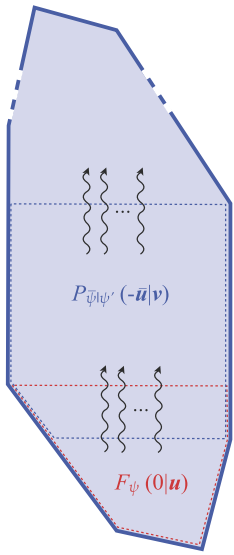

Fig. 1. A generic polygon tessellated into a sequence of pentagon transitions (shown by dashed contours) between eigenstates of the color flux tube. The bottom pentagon is encoded by the form factor for creation of corresponding excitations. Crossing relates it to pentagons.

$$P(u_1,\ldots,u_n|v_1,\ldots,v_m)=\frac{\prod_{i=1}^n\prod_{j=1}^m P(u_i|v_j)}{\prod_{i>j}^n P(u_i|u_j)\prod_{k<l}^m P(v_k|v_l)}\,, \tag{3}$$

where the transition is not necessarily particle number-preserving, i.e., $n\neq m$. This was verified for $n=m$ at leading order in Ref. [31] by mapping out the problem of interacting flux-tube excitations to an integrable spin chain with open boundary conditions [32,33]. Presently, the multiparticle pentagons will not be restricted to particles of the same type, however, the factorized form (3) will still stand strong. We will find that the same form is valid for fermions as well where the bootstrap equations are nonlinear. Apart from testing the factorized form, another goal of our consideration will be to confirm all pentagons introduced in previous analyses. To verify our findings, we will confront them against explicit data on multiparticle non-maximally helicity violating (non-MHV) amplitudes. To date, the only available source of the latter[3] is the package by Bourjaily–Caron-Huot–Trnka [35] that provides amplitudes to one-loop order. The main observable will be the ratio function

$$\mathcal{P}_{N;n}=\mathcal{A}_{N;n}/\mathcal{A}_{N;0}\,, \tag{4}$$

of N^nMHV superamplitude $\mathcal{A}_{N;n}$ to maximally helicity violating (MHV) one $\mathcal{A}_{N;0}$.

Our subsequent presentation will be organized as follows. In the next section, we will focus on the heptagon. We construct a properly subtracted observable from the ratio function that is compared with results deduced from OPE. Since, there is one intermediate pentagon in this case, we will address successively single-particle, two-to-one and two-to-two transitions in turn. This case alone already encompasses all major flux-tube excitations. Eventually, we take a first look into three-particle transitions using a specific example. Next, we analyze octagons following the

[3] With the exception of the available symbol for two-loop NMHV heptagon derived in Ref. [34].

same footsteps in Section 3. Finally, we conclude. Several appendices are dedicated to provide details of computations performed in the main body. Appendix A exhibits the construction of reference polygons and the way all inequivalent polygons are parametrized. In Appendix B, we summarize all ingredients of the pentagon approach, i.e., all pentagon transitions, single and two-particle measures, in the latter case involving one small fermion, as well as flux-tube dispersion relations limiting ourselves to one-loop order.

2. Heptagon observable

As we pointed out in the Introduction, the hexagon was exhaustively studied in the literature to a very high order in 't Hooft coupling. Therefore, to start our present consideration, let us introduce a seven particle observable that we will be comparing our OPE predictions with. For the case at hand, there are two sets of conformal cross ratios τ_i, σ_i and ϕ_i $(i = 1, 2)$ which define momentum twistors parametrizing inequivalent heptagons (A.14), as discussed in Appendix A.

While the ratio function $\mathcal{P}_{7;n}$ in Eq. (4) is finite, the OPE frameworks provides predictions for a finite quantity which is constructed by factoring out the (inverse) bosonic Wilson loop from the former, namely,

$$\mathcal{W}_{7;n} = g^{2n}\mathcal{P}_{7;n}W_7\,, \tag{5}$$

where, obviously $\mathcal{P}_{7;0} = 1$ and the power of the 't Hooft coupling was introduced to match the definition of the expectation value of the supersymmetric Wilson loop of Refs. [8,7,9], according to which a tree NMHV amplitude corresponds to a one-loop expression on the Wilson loop side, N^2MHV to two-loop graphs etc. Above, W_7 is the heptagon observable that does not depend on the Grassmann variables, $W_7 = \mathcal{W}_{7;0}$, and can be split to all orders in 't Hooft coupling as

$$W_7 = W_7^{\mathrm{U}(1)}\exp(R_7)\,, \tag{6}$$

with $W_7^{\mathrm{U}(1)}$ being the sum of connected correlators between reference squares in a chosen tessellation of the heptagon calculated in U(1) theory[4] with the coupling constant $g^2_{\mathrm{U}(1)}$ being replaced by the cusp anomalous dimension $g^2_{\mathrm{U}(1)} = \frac{1}{4}\Gamma_{\mathrm{cusp}}(g^2)$ of the full theory [36] and a remainder function R_7. Since in the bulk of the paper we will not go beyond the first subleading order in g^2 due to the lack of higher loop data for multiparticle amplitudes, we ignore R_7, which starts at two loops [20,21], and use the following expansion that will suffice for our subsequent calculations

$$W_7^{\mathrm{U}(1)} = 1 + g^2\left[r_1(\tau_1,\sigma_1,\phi_1) + r_1(\tau_2,\sigma_2,\phi_2) + r_2(\tau_1,\tau_2,\sigma_1,\sigma_2,\phi_1,\phi_2)\right] + O(g^4)\,. \tag{7}$$

The reason for decomposing the order g^2 contribution in terms of three functions is that they have a clear representation via single-gluon exchanges between reference squares of the abelian Wilson loop [36]. At large τ, they develop the following decomposition

$$r_1(\tau,\sigma,\phi) = \mathrm{e}^{-\tau}(\mathrm{e}^{i\phi} + \mathrm{e}^{-i\phi})r_{1[1]}(\sigma) + \mathrm{e}^{-2\tau}(\mathrm{e}^{2i\phi} + \mathrm{e}^{-2i\phi})r_{1[2]}(\sigma) + \dots\,. \tag{8}$$

Here $r_{1[n]}$ is a twist-n contribution that admits an OPE interpretation in terms of single and two-gluon bound state, respectively, in the hexagon expansion (or, for the case of the heptagon, as a transition between the flux-tube excitations and the vacuum),

[4] See Eq. (127) in Ref. [14].

$$r_{1[1]}(\sigma)=\frac{1}{g^2}\int d\mu_{\rm g}(u)\,,\qquad r_{1[2]}(\sigma)=\frac{1}{g^2}\int d\mu_{D\rm g}(u)\,. \tag{9}$$

Their perturbative expansion $r=\sum_{\ell\geq 1}g^{2\ell}r^{(\ell)}$ starts at order g^2 and reads[5] at leading order in coupling [36,15]

$$r^{(1)}_{1[1]}(\sigma)=\pi\int\frac{du}{2\pi}\frac{-{\rm e}^{2iu\sigma}}{(u^2+\frac{1}{4})\cosh(\pi u)}=2\sigma{\rm e}^{\sigma}-2\cosh(\sigma)\ln(1+{\rm e}^{2\sigma})\,, \tag{10}$$

$$r^{(1)}_{1[2]}(\sigma)=\pi\int\frac{du}{2\pi}\frac{u\,{\rm e}^{2iu\sigma}}{(u^2+1)\sinh(\pi u)}=-\frac{1}{2}-\sigma{\rm e}^{2\sigma}+\cosh(2\sigma)\ln(1+{\rm e}^{2\sigma})\,, \tag{11}$$

making use of the explicit measures summarized in Appendix B. Analogously, the function $r_2(\tau_1,\tau_2,\sigma_1,\sigma_2,\phi_1,\phi_2)$ that depends on all heptagon variables emerges from the gluon exchange between the top and bottom reference squares and can be expressed in the near-collinear limit [39]

$$r_2(\tau_1,\tau_2,\sigma_1,\sigma_2,\phi_1,\phi_2)={\rm e}^{-\tau_1-\tau_2}({\rm e}^{i\phi_1+i\phi_2}+{\rm e}^{-i\phi_1-i\phi_2})r_{2[2]}(\sigma_1,\sigma_2)+\dots\,, \tag{12}$$

as a gauge field propagating on the flux tube with

$$r_{2[2]}(\sigma_1,\sigma_2)=\frac{1}{g^2}\int d\mu_{\rm g}(u)P_{\rm g|g}(-u|v)d\mu_{\rm g}(v)\,, \tag{13}$$

involving one intermediate gauge-field pentagon[6] $P_{\rm g|g}$ [3]. All helicity-violating contributions were not mentioned above since they arise in perturbation theory starting from two-loop order.

Our focus will be on the NMHV amplitudes $\mathcal{P}_{7;1}$. In what follows, we will introduce the following convention for the coefficients in the expansion of the heptagon super Wilson loop in a given OPE channel (where we omitted an overall Grassmann structure for each term in the series)

$$\mathcal{W}_{7;1}=\sum_{n_1,n_2}\sum_{h_1,h_2}{\rm e}^{-n_1\tau_1-n_2\tau_2}{\rm e}^{i(h_1\phi_1+h_2\phi_2)/2}\mathcal{W}_{[n_1,n_2](h_1,h_2)}(\sigma_1,\sigma_2;g)\,. \tag{14}$$

Here n_1 and n_2 stand the cumulative twists of excitations in the incoming and outgoing flux-tube states, while h_i stand for twice their corresponding helicities, $h_i=2m_i$. The function $\mathcal{W}_{[n_1,n_2](h_1,h_2)}(\sigma_1,\sigma_2;g)$ admits an infinite series expansion in 't Hooft coupling

$$\mathcal{W}_{[n_1,n_2](h_1,h_2)}(\sigma_1,\sigma_2;g)=g^2\sum_{\ell\geq 0}g^{2\ell}\mathcal{W}^{(\ell)}_{[n_1,n_2](h_1,h_2)}(\sigma_1,\sigma_2)\,. \tag{15}$$

As mentioned earlier, we pulled out a power of the coupling since the one-loop contribution $\mathcal{W}^{(0)}_{7;1}$ to the super Wilson loop is dual to the tree-level ratio function $\mathcal{P}^{(0)}_{7;1}$ [7–9]. Analogously, we will expand the ratio function $\mathcal{P}_{7;1}$,

$$\mathcal{P}_{7;1}=\sum_{n_1,n_2}\sum_{h_1,h_2}{\rm e}^{-n_1\tau_1-n_2\tau_2}{\rm e}^{i(h_1\phi_1+h_2\phi_2)/2}\mathcal{P}_{[n_1,n_2](h_1,h_2)}(\sigma_1,\sigma_2;g)\,, \tag{16}$$

with the perturbative series for accompanying coefficients being

[5] The emerging here and below one-loop Fourier transforms can be computed along the lines of Refs. [37,38].

[6] The first two terms in its perturbative expansion are given in Appendix B.

$$\mathcal{P}_{[n_1,n_2](h_1,h_2)}(\sigma_1,\sigma_2;g)=\sum_{\ell\geq 0} g^{2\ell}\mathcal{P}^{(\ell)}_{[n_1,n_2](h_1,h_2)}(\sigma_1,\sigma_2)\,. \tag{17}$$

As we alluded to above, the focus of the rest of this section will be on the NMHV contribution $\mathcal{W}_{7;1}$ to the superheptagon. The SU(4) symmetry fixes $\mathcal{W}_{7;1}$ to be a homogeneous SU(4) invariant polynomial in Grassmann variables χ_i^A $(i=1,\ldots,7)$ of degree 4. Thus it admits the following Grassmann expansion

$$\begin{aligned}
\mathcal{W}_{7;1}=\chi_1^2\chi_4^2\Big\{&\mathrm{e}^{-\tau_1-\tau_2}\mathcal{W}_{[1,1](0,0)}\\
&+\mathrm{e}^{-2\tau_1-\tau_2}\mathrm{e}^{i\phi_1}\mathcal{W}_{[2,1](2,0)}+\mathrm{e}^{-2\tau_1-\tau_2}\mathrm{e}^{-i\phi_1}\mathcal{W}_{[2,1](-2,0)}\\
&+\mathrm{e}^{-2\tau_1-2\tau_2}\Big[\mathrm{e}^{-i\phi_1+i\phi_2}\mathcal{W}_{[2,2](-2,2)}+\ldots\Big]+\ldots\Big\}\\
&+\chi_1^3\chi_4\Big\{\mathrm{e}^{-\tau_1-\tau_2}\mathrm{e}^{i\phi_1/2+i\phi_2/2}\mathcal{W}_{[1,1](1,1)}\\
&+\mathrm{e}^{-2\tau_1-\tau_2}\Big[\mathrm{e}^{3i\phi_1/2+i\phi_2/2}\mathcal{W}_{[2,1](3,1)}+\mathrm{e}^{-i\phi_1/2+i\phi_2/2}\mathcal{W}_{[2,1](-1,1)}\Big]\\
&+\mathrm{e}^{-2\tau_1-2\tau_2}\Big[\mathrm{e}^{3i\phi_1/2+3i\phi_2/2}\mathcal{W}_{[2,2](3,3)}+\mathrm{e}^{-i\phi_1/2+3i\phi_2/2}\mathcal{W}_{[2,2](-1,3)}+\ldots\Big]\\
&+\mathrm{e}^{-3\tau_1-\tau_2}\Big[\mathrm{e}^{-3i\phi_1/2+i\phi_2/2}\mathcal{W}_{[3,1](-3,1)}+\ldots\Big]+\ldots\Big\}\\
&+\ldots\,,
\end{aligned} \tag{18}$$

where $\chi_1^2\chi_4^2=\varepsilon_{ABCD}\chi_1^A\chi_1^B\chi_4^C\chi_4^D$ etc. Here we only displayed terms in the OPE that form a representative class of contributions that will be the subject of the current analysis. The χ_i^4 contributions were considered previously in Ref. [17] and thus to avoid repetition will not be discussed below.

2.1. One-to-one transitions

We start our consideration with the $\chi_1^2\chi_4^2$ component. The leading twist contribution is determined by the exchange of the hole excitation propagating on the color flux tube and, as was established in Ref. [14], it reads

$$\mathcal{W}_{[1,1](0,0)}=-\int d\mu_{\mathrm{h}}(u)\,P_{\mathrm{h}|\mathrm{h}}(-u|v)d\mu_{\mathrm{h}}(v)\,. \tag{19}$$

To lowest order in perturbative series, it takes the form

$$\begin{aligned}
\mathcal{W}^{(0)}_{[1,1](0,0)}(\sigma_1,\sigma_2)&=\mathcal{P}^{(0)}_{[1,1](0,0)}(\sigma_1,\sigma_2)\\
&=-\pi^2\int\frac{du}{2\pi}\frac{dv}{2\pi}\frac{\mathrm{e}^{2i\sigma_1 u+2i\sigma_2 v}}{\cosh(\pi u)\cosh(\pi v)}\frac{\Gamma(-iu-iv)}{\Gamma(\frac{1}{2}-iu)\Gamma(\frac{1}{2}-iv)}\\
&=-\frac{\mathrm{e}^{\sigma_1+\sigma_2}}{\mathrm{e}^{2\sigma_1}+\mathrm{e}^{2\sigma_2}+\mathrm{e}^{2\sigma_1+2\sigma_2}}\,,
\end{aligned} \tag{20}$$

making use of results summarized in Appendix B. It agrees with the expression for the ratio function $\mathcal{P}^{(0)}_{[1,1](0,0)}$ deduced from the package [35]. The subleading correction in 't Hooft coupling agrees as well. We do not display it explicitly here in order to save space (see, however, the ancillary file).

Next, we turn to the $\chi_1^3\chi_4$ component of the heptagon. As can be easily anticipated on the basis of quantum numbers by counting the fermionic degree and SU(4) weight of the accompanying Grassmann structure, the leading term in the near-collinear expansion is governed by the exchange of the fermionic flux-tube excitation, namely,

$$\mathcal{W}_{[1,1](1,1)} = -i \int d\mu_\Psi(u_1) x[u_1] P_{\Psi|\Psi}(-u_1|v_1)\, d\mu_\Psi(v_1)\,, \tag{21}$$

where $x[u]$ is an ad hoc NMHV fermionic form factor [15,16,18] given by the Zhukowski variable whose definition is deferred to Eq. (B.45) of Appendix B. Here the contour C runs on both the large and small fermion sheets of the corresponding Riemann surface, as was reviewed in the Introduction. Since there are no poles in the integrand on the small fermion sheet, its contribution vanishes identically. This can be understood recalling that the small fermion at zero momentum is a generator of supersymmetric transformation [40]. Since for the case at hand, it is the only excitation present on the top or the bottom of the heptagon, it would correspond to the action of the supersymmetry generator on the vacuum state and thus yield vanishing net result. Hence, the above super Wilson loop component reads in the OPE framework

$$\mathcal{W}_{[1,1](1,1)} = -i \int d\mu_{\rm F}(u) x[u] P_{\rm F|F}(-u|v) d\mu_{\rm F}(v)\,. \tag{22}$$

Taylor expanding all ingredients in 't Hooft coupling, we immediately reproduce the tree-level $\chi_1^3\chi_4$ contribution to the ratio function

$$\begin{aligned}\mathcal{W}^{(0)}_{[1,1](1,1)}(\sigma_1,\sigma_2) &= \mathcal{P}^{(0)}_{[1,1](1,1)}(\sigma_1,\sigma_2)\\ &= -\pi^2 \int \frac{du_1}{2\pi}\frac{dv_1}{2\pi}\frac{e^{2i\sigma_1 u_1+2i\sigma_2 v_1}}{\sinh(\pi u_1)\sinh(\pi v_1)}\frac{\Gamma(-iu_1-iv_1)}{\Gamma(-iu_1)\Gamma(1-iv_1)}\\ &= \frac{e^{2\sigma_1}}{(1+e^{2\sigma_1})(e^{2\sigma_1}+e^{2\sigma_2}+e^{2\sigma_1+2\sigma_2})}\,.\end{aligned} \tag{23}$$

Substituting perturbative expansions quoted in Appendix B, this agreement can be extended to one loop order as well (see the accompanying Mathematica notebook).

Analogously, if we were to consider the $\chi_1\chi_4^3$ component, one would find that the leading twist contribution is determined by the permutation transformation of the $\chi_1^3\chi_4$ contribution, i.e., $\mathcal{W}_{[1,1](-1,-1)}(\sigma_1,\sigma_2;g) = \mathcal{W}_{[1,1](1,1)}(\sigma_2,\sigma_1;g)$ and reads explicitly,

$$\mathcal{W}_{[1,1](-1,-1)} = -i \int d\mu_{\rm F}(u) P_{\rm F|F}(-u|v) x[v] d\mu_{\rm F}(v)\,. \tag{24}$$

2.2. Two-to-one transitions

Let us move on to two-particle states. We begin our discussion of twist-two contributions with the particle number-changing case when the bottom part of the heptagon emits two flux-tube excitations while the top absorbs only one. We will observe on a number of examples that the two-to-one pentagons factorize in terms of single-particle ones as follows[7]

$$P_{\rm p_1p_2|p_3}(u_1,u_2|v_1) = \frac{P_{\rm p_1|p_3}(u_1|v_1)P_{\rm p_2|p_3}(u_2|v_1)}{P_{\rm p_2|p_1}(u_2|u_1)}\,. \tag{25}$$

[7] We do not display potential kinematical SU(4) tensor structure but focus only on the dynamical part of pentagon transitions.

The above expression follows the pattern of gluonic transitions conjectured in Ref. [3] and verified at leading order in Ref. [31], however, here it is not restricted to particles of the same type. We will find that the same form is valid for fermions where the bootstrap equations are nonlinear [15,18].

2.2.1. Two-(anti)fermion and scalar-(anti)gluon states

To analyze the two-(anti)fermion and scalar-(anti)gluon states, we turn to the twist-two contribution in the $\chi_1^2\chi_4^2$ Grassmann component. The operator product expansion for $\mathcal{W}_{[2,1](2,0)}$ is related to the properly defined ratio function (5) as follows

$$\mathcal{W}^{(0)}_{[2,1](2,0)}(\sigma_1,\sigma_2)=\mathcal{P}^{(0)}_{[2,1](2,0)}(\sigma_1,\sigma_2)\,, \tag{26}$$

$$\mathcal{W}^{(1)}_{[2,1](2,0)}(\sigma_1,\sigma_2)=\mathcal{P}^{(1)}_{[2,1](2,0)}(\sigma_1,\sigma_2)+\mathcal{P}^{(0)}_{[1,1](0,0)}(\sigma_1,\sigma_2)r^{(1)}_{1[1]}(\sigma_1)\,, \tag{27}$$

at tree and one-loop order, respectively. These arise from the sum of two particles that mimic the quantum numbers of a hole in the in-state and a single hole in the outgoing state, such that

$$\mathcal{W}_{[2,1](2,0)}=\mathcal{W}_{\Psi\Psi|\mathrm{h}}+\mathcal{W}_{\mathrm{gh}|\mathrm{h}}\,, \tag{28}$$

with

$$\mathcal{W}_{\Psi\Psi|\mathrm{h}}=\int d\mu_\Psi(u_1)d\mu_\Psi(u_2)\frac{x[u_1]}{g^2}\frac{x[u_2]}{g^2}F^{\mathbf{6}}_{\Psi\Psi}(0|u_1,u_2)P_{\Psi\Psi|\mathrm{h}}(-u_2,-u_1|v_1)d\mu_{\mathrm{h}}(v_1)\,, \tag{29}$$

$$\mathcal{W}_{\mathrm{gh}|\mathrm{h}}=\int d\mu_{\mathrm{g}}(u_1)d\mu_{\mathrm{h}}(u_2)\frac{\sqrt{x^+[u_1]x^-[u_1]}}{g}F_{\mathrm{gh}}(0|u_1,u_2)P_{\mathrm{hg}|\mathrm{h}}(-u_2,-u_1|v_1)d\mu_{\mathrm{h}}(v_1), \tag{30}$$

where the two-particle production form factors are [16,18]

$$F^{\mathbf{6}}_{\Psi\Psi}(0|u_1,u_2)=\frac{i}{u_1-u_2+i}\frac{1}{P_{\Psi|\Psi}(u_1|u_2)}\,,\qquad F_{\mathrm{gh}}(0|u_1,u_2)=\frac{i}{P_{\mathrm{g}|\mathrm{h}}(u_1|u_2)}\,. \tag{31}$$

In the course of the study, we established the following empirical rule for introduction of additional "helicity" form factors, whenever the intermediate pentagon transitions $P_{\mathrm{p}_1,\mathrm{p}_2,\ldots|\mathrm{p}'_1,\mathrm{p}'_2,\ldots}$ involved (anti)gluons, $\mathrm{p}_i,\mathrm{p}'_j=\mathrm{g},\bar{\mathrm{g}}$. Namely, for each pair in the product of all permutations $\sigma=\{1,2,\ldots\}$ and $\sigma'=\{1',2',\ldots\}$ of in-out state transitions $\mathrm{p}_\sigma|\mathrm{p}'_{\sigma'}$, we introduced extra factors depending on the shifted Zhukowski variables (B.46) according to the rule

$$\langle \mathrm{g}(u)|\,,|\bar{\mathrm{g}}(u)\rangle\to\frac{g}{\sqrt{x^+[u]x^-[u]}}\,,\qquad \langle\bar{\mathrm{g}}(u)|\,,|\mathrm{g}(u)\rangle\to\frac{\sqrt{x^+[u]x^-[u]}}{g}\,, \tag{32}$$

when the in/out state contained an (anti)gluon, and the conjugate one had a hole and an (anti)fermion. This compensated the square-root factors emerging in the solution to bootstrap equations in the conventions of Refs. [16,18].

In the same fashion as in the previously addressed twist-one case, the fermionic contour runs on both sheets of the Riemann surface. Presently, the leading effect arises, however, from the kinematics when one of the rapidities belongs to the small sheet and another to the large one. Since $F^{\mathbf{6}}_{\mathrm{fF}}(0|u_1,u_2)$ has a pole in the lower half plane at $u_1=u_2-i$, one can evaluate the integral over u_1 using the Cauchy theorem. Thus $\mathcal{W}_{\Psi\Psi|\mathrm{h}}$ splits up into the sum of two contributions, $\mathcal{W}_{\Psi\Psi|\mathrm{h}}=\mathcal{W}_{\mathrm{fF}|\mathrm{h}}+\mathcal{W}_{\mathrm{FF}|\mathrm{h}}$,

$$\mathcal{W}_{\mathrm{fF|h}} = \frac{1}{g^2}\int d\mu_{\mathrm{fF}}(u_2)\, P_{\mathrm{f|h}}(-u_2+i|v_1)\, P_{\mathrm{F|h}}(-u_2|v_1) d\mu_{\mathrm{h}}(v_1)\,, \tag{33}$$

$$\mathcal{W}_{\mathrm{FF|h}} = \frac{1}{g^4}\int d\mu_{\mathrm{F}}(u_1) d\mu_{\mathrm{F}}(u_2) \frac{i x[u_1] x[u_2]\, P_{\mathrm{F|h}}(-u_1|v_1)\, P_{\mathrm{F|h}}(-u_2|v_1)}{(u_1-u_2+i)\, P_{\mathrm{F|F}}(u_1|u_2)\, P_{\mathrm{F|F}}(-u_1|-u_2)} d\mu_{\mathrm{h}}(v_1)\,, \tag{34}$$

of the small–large and large–large fermion pairs, respectively. In the former, we employed a notation for the composite two-fermion measure [16]

$$\mu_{\mathrm{fF}}(u) = -\frac{x[u]}{x[u-i]}\frac{\mu_{\mathrm{f}}(u-i)\mu_{\mathrm{F}}(u)}{P_{\mathrm{f|F}}(u-i|u) P_{\mathrm{f|F}}(-u+i|-u)}\,. \tag{35}$$

It is important to recall that as one passes to the small fermion sheet, the Zhukowski variable x transforms to g^2/x [12]. Equation (33) accounts for the entire tree-level NMHV ratio function as it starts at order g^2,

$$\begin{aligned}\mathcal{W}^{(0)}_{[2,1](2,0)}(\sigma_1,\sigma_2) &= \mathcal{W}^{(0)}_{\mathrm{fF|h}}(\sigma_1,\sigma_2)\\ &= \pi^2\int \frac{du_2}{2\pi}\frac{dv_1}{2\pi}\frac{\mathrm{e}^{2iu_2\sigma_1+2iv_1\sigma_2}}{\sinh(\pi u_2)\cosh(\pi v_1)}\frac{i\Gamma(\frac{1}{2}-iu_2-iv_1)}{\Gamma(-iu_2)\Gamma(\frac{1}{2}-iv_1)}\\ &= \frac{\mathrm{e}^{2\sigma_1+3\sigma_2}}{(\mathrm{e}^{2\sigma_1}+\mathrm{e}^{2\sigma_2}+\mathrm{e}^{2\sigma_1+2\sigma_2})^2}\,.\end{aligned} \tag{36}$$

While the second one, $\mathcal{W}_{\mathrm{FF|h}}$, is postponed to $O(g^4)$. Notice that the latter contributes to the Wilson loop an order earlier in 't Hooft coupling compared to the hexagon [16]. In addition, the one-loop ratio function (27) receives an additive contribution from the incoming gluon–hole state,

$$\mathcal{W}_{\mathrm{gh|h}} = \frac{1}{g}\int d\mu_{\mathrm{g}}(u_1) d\mu_{\mathrm{h}}(u_2) \frac{i\sqrt{x^+[u_1]x^-[u_1]}\, P_{\mathrm{g|h}}(-u_1|v_1)\, P_{\mathrm{h|h}}(-u_2|v_1)}{P_{\mathrm{g|h}}(u_1|u_2)\, P_{\mathrm{g|h}}(-u_1|-u_2)} d\mu_{\mathrm{h}}(v_1)\,. \tag{37}$$

Combining $\mathcal{W}^{(1)}_{\mathrm{fF|h}}$, $\mathcal{W}^{(1)}_{\mathrm{FF|h}}$ and $\mathcal{W}^{(1)}_{\mathrm{gh|h}}$ together, we uncover the one-loop NMHV amplitude (27) as demonstrated in the accompanying Mathematica notebook.

The two-antifermion states emerge in the $\mathcal{W}_{[2,1](-2,0)}$ component of the superloop. This transition will be sensitive to the hole–antifermion pentagons. Since the bosonic Wilson loop is symmetric with respect to the flip in sign of the gluon helicity, i.e., $\phi_1 \leftrightarrow -\phi_1$, the subtracted ratio function takes the same form as above Eqs. (26) and (27) with obvious substitutions $\mathcal{W}^{(\ell)}_{[2,1](2,0)} \to \mathcal{W}^{(\ell)}_{[2,1](-2,0)}$. These arise from the sum of two-particles in the in-state and a single hole in the outgoing state, such that

$$\mathcal{W}_{[2,1](-2,0)} = \mathcal{W}_{\bar\Psi\bar\Psi|\mathrm{h}} + \mathcal{W}_{\bar{\mathrm{g}}\mathrm{h}|\mathrm{h}}\,, \tag{38}$$

with

$$\mathcal{W}_{\bar\Psi\bar\Psi|\mathrm{h}} = \frac{1}{g^2}\int d\mu_\Psi(u_1) d\mu_\Psi(u_2) F^{\mathbf{6}}_{\Psi\Psi}(0|u_1,u_2)\, P_{\bar\Psi\bar\Psi|\mathrm{h}}(-u_2,-u_1|v_1) d\mu_{\mathrm{h}}(v_1)\,, \tag{39}$$

$$\mathcal{W}_{\bar{\mathrm{g}}\mathrm{h}|\mathrm{h}} = \int d\mu_{\mathrm{g}}(u_1) d\mu_{\mathrm{h}}(u_2) \frac{g F_{\bar{\mathrm{g}}\mathrm{h}}(0|u_1,u_2)}{\sqrt{x^+[u_1]x^-[u_1]}} P_{\mathrm{h}\bar{\mathrm{g}}|\mathrm{h}}(-u_2,-u_1|v_1) d\mu_{\mathrm{h}}(v_1)\,. \tag{40}$$

However, an immediate inspection demonstrates that to one-loop accuracy, the small–large antifermion pair alone accommodates the entire contribution in the operator product expansion such that to this accuracy $\mathcal{W}_{[2,1](-2,0)}$ reads

$$\mathcal{W}_{[2,1](-2,0)} = \mathcal{W}_{\bar{\mathrm{f}}\mathrm{F}|\mathrm{h}} + O(g^6)$$
$$= \frac{1}{g^2}\int d\mu_{\mathrm{fF}}(u_2)\frac{x[u_2-i]}{x[u_2]}P_{\mathrm{f}|\mathrm{h}}(-u_2+i|v_1)P_{\mathrm{F}|\mathrm{h}}(-u_2|v_1)d\mu_{\mathrm{h}}(v_1) + O(g^6)\,. \tag{41}$$

Perturbative expansion yields for the tree amplitude

$$\mathcal{W}^{(0)}_{[2,1](-2,0)} = \mathcal{W}^{(0)}_{\bar{\mathrm{f}}\mathrm{F}|\mathrm{h}} = \pi^2\int\frac{du_2}{2\pi}\frac{dv_1}{2\pi}\frac{\mathrm{e}^{2iu_2\sigma_1+2iv_1\sigma_2}}{\sinh(\pi u_2)\cosh(\pi v_1)}\frac{(u_2-i)\Gamma(\frac{1}{2}-iu_2-iv_1)}{\Gamma(1-iu_2)\Gamma(\frac{1}{2}-iv_1)}$$
$$= -\frac{\mathrm{e}^{5\sigma_2}}{(1+\mathrm{e}^{2\sigma_2})(\mathrm{e}^{2\sigma_1}+\mathrm{e}^{2\sigma_2}+\mathrm{e}^{2\sigma_1+2\sigma_2})^2}\,. \tag{42}$$

Further expansion in 't Hooft coupling making use of explicit integrability input from Appendix B shows that this small–large antifermion pair solely accounts for $\mathcal{W}^{(1)}_{[2,1](-2,0)}$ as well. The true two-particle contribution get pushed to two-loop order similarly to the phenomenon observed for the NMHV hexagon [16,18].

2.2.2. Antifermion–hole states

The above consideration exhausted the two-to-one transitions to the $\chi_1^2\chi_4^2$ Grassmann component, thus we turn without further ado to the $\chi_1^3\chi_4$ contribution. The quantum numbers of states propagating in this OPE channel suggest that $\mathcal{W}_{[2,1](-1,1)}$ is determined by the sum of an antifermion–hole and antigluon–fermion produced at the bottom of the Wilson loop,

$$\mathcal{W}_{[2,1](-1,1)} = \mathcal{W}_{\bar{\Psi}\mathrm{h}|\Psi} + \mathcal{W}_{\Psi\bar{\mathrm{g}}|\Psi}\,. \tag{43}$$

Their explicit all-order expression is given by

$$\mathcal{W}_{\bar{\Psi}\mathrm{h}|\Psi} = \int d\mu_\Psi(u_1)\,d\mu_{\mathrm{h}}(u_2)\,\frac{ix[u_1]}{g}F^{\mathbf{4}}_{\bar{\Psi}\mathrm{h}}(0|u_1,u_2)P_{\mathrm{h}\bar{\Psi}|\Psi}(-u_2,-u_1|v_1)\,d\mu_\Psi(v_1)\,, \tag{44}$$

$$\mathcal{W}_{\Psi\bar{\mathrm{g}}|\Psi} = \int d\mu_\Psi(u_1)\,d\mu_{\mathrm{g}}(u_2)\,ix[u_1]\frac{gF_{\Psi\bar{\mathrm{g}}}(0|u_1,u_2)}{\sqrt{x^+[u_2]x^-[u_1]}}P_{\bar{\mathrm{g}}\Psi|\Psi}(-u_2,-u_1|v_1)\,d\mu_\Psi(v_1)\,. \tag{45}$$

Here an (anti)gluon accompanies a flux-tube fermion as a consequence, we introduced an additional form factor according to the rule (32). In our previous studies [18], we found that the form factor $F^{\mathbf{4}}_{\bar{\Psi}\mathrm{h}}(0|u_1,u_2)$ possesses a pole in the lower half-plane of the small fermion Riemann sheet, while the $F_{\Psi\bar{\mathrm{g}}}(0|u_1,u_2)$ one does not. This implies that $\mathcal{W}_{\bar{\Psi}\mathrm{h}|\Psi}$ at least induces the entire tree-level ratio function $\mathcal{P}^{(0)}_{[2,1](-1,1)}$. Substituting

$$F^{\mathbf{4}}_{\bar{\Psi}\mathrm{h}}(0|u_1,u_2) = \frac{1}{u_1-u_2+\frac{3i}{2}}\frac{1}{P_{\bar{\Psi}|\mathrm{h}}(u_1|u_2)}\,, \tag{46}$$

and splitting $\mathcal{W}_{\bar{\Psi}\mathrm{h}|\Psi}$ into the sum of the small and large fermions in the initial state, $\mathcal{W}_{\bar{\Psi}\mathrm{h}|\Psi} = \mathcal{W}_{\bar{\mathrm{f}}\mathrm{h}|\mathrm{F}} + \mathcal{W}_{\bar{\mathrm{F}}\mathrm{h}|\mathrm{F}}$, we find that $\mathcal{W}_{\bar{\mathrm{f}}\mathrm{h}|\mathrm{F}}$, that reads

$$\mathcal{W}_{\bar{\mathrm{f}}\mathrm{h}|\mathrm{F}} = -\frac{1}{g}\int d\mu_{\mathrm{fh}}(u_2)P_{\mathrm{f}|\mathrm{F}}(-u_2+\tfrac{3i}{2}|v_1)P_{\mathrm{h}|\mathrm{F}}(-u_2|v_1)d\mu_{\mathrm{F}}(v_1)\,, \tag{47}$$

actually does account for both tree and one-loop subtracted ratio function (5). Here we used a notation for the composite small-antifermion–hole measure [18]

$$\mu_{\rm hf}(u)=\frac{g^2}{x[u-\frac{3i}{2}]}\frac{\mu_{\rm h}(u)\mu_{\rm f}(u-\frac{3i}{2})}{P_{\rm h|f}\left(u|u-\frac{3i}{2}\right)P_{\rm h|f}\left(-u|-u+\frac{3i}{2}\right)}\,. \tag{48}$$

Employing its perturbative expansion summarized in Appendix B, we find

$$\begin{aligned}\mathcal{W}^{(0)}_{[2,1](-1,1)}=\mathcal{W}^{(0)}_{\rm fh|F}&=\pi^2\int\frac{du_2}{2\pi}\frac{dv_1}{2\pi}\frac{e^{2iu_2\sigma_1+2iv_1\sigma_2}}{\cosh(\pi u_2)\sinh(\pi v_1)}\frac{(u_2-\frac{3i}{2})\Gamma(\frac12-iu_2-iv_1)}{\Gamma(\frac12-iu_2)\Gamma(1-iv_1)}\\&=-\frac{e^{3\sigma_1}(2e^{2\sigma_1}+e^{4\sigma_1}+3e^{2\sigma_2}+4e^{2\sigma_1+2\sigma_2}+e^{4\sigma_1+2\sigma_2})}{(1+e^{2\sigma_1})^2(e^{2\sigma_1}+e^{2\sigma_2}+e^{2\sigma_1+2\sigma_2})^2}\,.\end{aligned} \tag{49}$$

We also observed agreement for $\mathcal{W}^{(1)}_{[2,1](-1,1)}$ at one loop order (see the ancillary file). This implies that contributions from the large-antifermion–hole and antigluon–fermion pairs cumulatively vanish at this order.

2.2.3. *Fermion–gluon states*

We continue the analysis of the $\chi_1^3\chi_4$ component by unraveling the structure of its $\mathcal{W}_{[2,1](3,1)}$ term. The tree and one-loop coefficients in the perturbative expansion of the latter are related to the ratio function via Eqs. (26) and (27) with $\mathcal{W}^{(\ell)}_{[2,1](2,0)}$ replaced by $\mathcal{W}^{(\ell)}_{[2,1](3,1)}$ and $\mathcal{P}^{(0)}_{[1,1](0,0)}$ by $\mathcal{P}^{(0)}_{[1,1](1,1)}$. The analysis of quantum numbers suggests that this component is induced by the emission of the gluon–fermion pair at the bottom of the hexagon and absorption of a single fermion at the top. Thus its all-order expression reads

$$\begin{aligned}\mathcal{W}_{[2,1](3,1)}=\mathcal{W}_{\Psi{\rm g}|\Psi}=\int d\mu_\Psi(u_1)\,d\mu_{\rm g}(u_2)\,ix[u_1]\,\frac{\sqrt{x^+[u_2]x^-[u_2]}}{g}\\ \times F_{\Psi{\rm g}}(0|u_1,u_2)P_{{\rm g}\Psi|\Psi}(-u_2,-u_1|v_1)\,d\mu_\Psi(v_1)\,.\end{aligned} \tag{50}$$

Here the form factor for the production of the Ψg state is

$$F_{\Psi{\rm g}}(0|u_1,u_2)=\frac{1}{P_{\Psi|{\rm g}}(u_1|u_2)}\,. \tag{51}$$

The fermion contour runs over the large and small fermion sheets such that

$$\mathcal{W}_{[2,1](3,1)}=\mathcal{W}_{\rm fg|F}+\mathcal{W}_{\rm Fg|F}\,. \tag{52}$$

Due to a zero in the small-fermion pentagon $P_{\rm f|g}(u_1|u_2)$, the corresponding form factor possesses a pole at $u_1=u_2-\frac{i}{2}$ in the lower half plane of the small fermion Riemann sheet. Evaluating the integral over the small fermion rapidity u_1, we obtain the expression

$$\mathcal{W}_{\rm fg|F}=\frac{1}{g}\int d\mu_{\rm fg}(u_2)\sqrt{x^+[u_2]x^-[u_2]}P_{\rm f|F}(-u_2+\tfrac{i}{2}|v_1)P_{\rm g|F}(-u_2|v_1)d\mu_{\rm F}(v_1)\,, \tag{53}$$

where we introduced, following Ref. [18], the composite fermion–gluon measure

$$\mu_{\rm fg}(u)=ig^2\frac{\mu_{\rm g}(u)\mu_{\rm f}(u^-)}{x[u^-]}\frac{f^{\bar{\rm g}\rm f}(u,u^-)f^{\bar{\rm g}\rm f}(-u,-u^-)}{P_{\bar{\rm g}|\rm f}(u|u^-)P_{\bar{\rm g}|\rm f}(-u|-u^-)}\,, \tag{54}$$

with $f^{\bar{\rm g}\rm f}(u,v)=(x^+[u]x[v]-g^2)(x^-[u]x[v]-g^2)/(g^2x[v])$. Making use of their Taylor expansion in coupling, one can easily convince oneself that the tree and one-loop terms of $\mathcal{W}_{\rm fg|F}$ reproduce the subtracted ratio function $\mathcal{W}_{[2,1](3,1)}$ with the leading term yielding explicitly

$$\mathcal{W}^{(0)}_{[2,1](3,1)} = \pi^2 \int \frac{du_2}{2\pi}\frac{dv_1}{2\pi}\frac{e^{2iu_2\sigma_1+2iv_1\sigma_2}}{\cosh(\pi u_2)\sinh(\pi v_1)}\frac{i\Gamma(\frac{1}{2}-iu_2-iv_1)}{\Gamma(-\frac{1}{2}-iu_2)\Gamma(1-iv_1)}$$
$$= -\frac{e^{3\sigma_1}(e^{2\sigma_1}+2e^{2\sigma_2}+2e^{2\sigma_1+2\sigma_2})}{(1+e^{2\sigma_1})^2(e^{2\sigma_1}+e^{2\sigma_2}+e^{2\sigma_1+2\sigma_2})^2}\,. \tag{55}$$

The contribution of the large fermion–gluon pair is postponed to two-loop order as verified in the accompanying notebook. The twist-one-to-twist-two transition in the $\chi_1\chi_4^3$ component, i.e., $e^{-\tau_1-2\tau_2}e^{-i\phi_1/2-3i\phi_2/2}$ is eagerly obtained from the above by the $\sigma_1 \leftrightarrow \sigma_2$ interchange.

2.3. Two-to-two transitions

To elucidate the factorizability of multiparticle pentagons even further, let us address a couple of examples involving two-to-two transitions. For these, the dynamical part of multiparticle pentagons will be assumed to admit the following form, echoing Eq. (3),

$$P_{p_1p_2|p_3p_4}(u_1,u_2|v_1,v_2) = \frac{P_{p_1|p_3}(u_1|v_1)P_{p_2|p_3}(u_2|v_1)P_{p_1|p_4}(u_1|v_2)P_{p_2|p_4}(u_2|v_2)}{P_{p_2|p_1}(u_2|u_1)P_{p_3|p_4}(v_1|v_2)}\,. \tag{56}$$

Let us offer a perturbative confirmation for this conjecture though a number of examples.

2.3.1. Two-(anti)fermion states

First, we will analyze the $\mathcal{W}_{[2,2](-2,2)}$ term in the $\chi_1^2\chi_4^2$ component of the superloop. The function $\mathcal{W}_{[2,2](-2,2)}$ can be split into the sum of four terms

$$\mathcal{W}_{[2,2](-2,2)} = \mathcal{W}_{\bar\Psi\bar\Psi|\Psi\Psi} + \mathcal{W}_{\bar g\bar h|\Psi\Psi} + \mathcal{W}_{\bar\Psi\bar\Psi|gh} + \mathcal{W}_{\bar g\bar h|gh}\,. \tag{57}$$

However, only the first term in the right-hand side induces a nontrivial contribution to the first two orders in the perturbative expansion of the ratio function as will be established momentarily. This two-antifermion-to-two-fermion transition admits the following form in terms of flux-tube pentagons

$$\mathcal{W}_{\bar\Psi\bar\Psi|\Psi\Psi} = \int d\mu_\Psi(u_1)d\mu_\Psi(u_2)\frac{x[u_1]}{g^2}\frac{x[u_2]}{g^2}F^{\mathbf{6}}_{\Psi\Psi}(0|u_1,u_2)$$
$$\times P_{\bar\Psi\bar\Psi|\Psi\Psi}(-u_2,-u_1|v_1,v_2)\frac{x[v_1]}{g^2}\frac{x[v_2]}{g^2}F^{\mathbf{6}}_{\Psi\Psi}(-v_2,-v_1|0)\mu_\Psi(v_1)d\mu_\Psi(v_2) \tag{58}$$

and can be split into four terms depending on whether the fermion rapidity belongs to the large or small fermion sheet. As a working hypothesis, the two-to-two particle pentagon will be taken in the factorized form (56). In the above formula, the absorption form factor is related to the emission one (31) via $F^{\mathbf{6}}_{\Psi\Psi}(-v_2,-v_1|0) = F^{\mathbf{6}}_{\Psi\Psi}(0|v_2,v_1)$. Since the two-fermion production/absorption form factors possess poles and the rest of the integrand is a holomorphic function, the integrals over the small fermion u_1 and v_2 rapidities can be worked out by calculating the residues at the position of the latter yielding

$$\mathcal{W}_{\bar{\mathrm{f}}\bar{\mathrm{F}}|\mathrm{Ff}} = \frac{1}{g^2}\int d\mu_{\mathrm{fF}}(u_2)P_{\bar{\mathrm{F}}|\mathrm{F}}(-u_2|v_1)P_{\bar{\mathrm{F}}|\mathrm{f}}(-u_2|v_1-i)P_{\bar{\mathrm{f}}|\mathrm{F}}(-u_2+i|v_1)$$
$$\times P_{\bar{\mathrm{f}}|\mathrm{f}}(-u_2+i|v_1-i)d\mu_{\mathrm{fF}}(v_1)\,. \tag{59}$$

Here the composite small–large fermion measure was quoted earlier in Eq. (35). Making use of the perturbative expansion summarized in Appendix B, we find a complete agreement with subtracted tree and one-loop ratio functions

$$\mathcal{W}^{(0)}_{[2,2](-2,2)}(\sigma_1,\sigma_2)=\mathcal{P}^{(0)}_{[2,2](-2,2)}(\sigma_1,\sigma_2)\,, \tag{60}$$

$$\begin{aligned}\mathcal{W}^{(1)}_{[2,2](-2,2)}(\sigma_1,\sigma_2)&=\mathcal{P}^{(1)}_{[2,2](-2,2)}(\sigma_1,\sigma_2)+\mathcal{P}^{(0)}_{[1,2](0,2)}(\sigma_1,\sigma_2)r^{(1)}_{1[1]}(\sigma_1)\\&\quad+\mathcal{P}^{(0)}_{[2,1](-2,0)}(\sigma_1,\sigma_2)r^{(1)}_{1[1]}(\sigma_2)\,.\end{aligned} \tag{61}$$

In particular, $\mathcal{W}_{[2,2](-2,2)}=\mathcal{W}_{\bar{\mathrm{f}}\bar{\mathrm{F}}|\mathrm{Ff}}+O(g^6)$, at leading order

$$\begin{aligned}&\mathcal{W}^{(0)}_{[2,2](-2,2)}\\&\quad=\mathcal{W}^{(0)}_{\bar{\mathrm{f}}\bar{\mathrm{F}}|\mathrm{Ff}}=-\pi^2\int\frac{du_2}{2\pi}\frac{dv_1}{2\pi}\frac{\mathrm{e}^{2iu_2\sigma_1+2iv_1\sigma_2}}{\sinh(\pi u_2)\sinh(\pi v_1)}\frac{(u_2-i)(v_1-i)\Gamma(1-iu_2-iv_1)}{\Gamma(1-iu_2)\Gamma(1-iv_1)}\\&\quad=-\frac{\mathrm{e}^{6\sigma_1}+3\mathrm{e}^{4\sigma_1+2\sigma_2}+5\mathrm{e}^{6\sigma_1+2\sigma_2}+6\mathrm{e}^{4\sigma_1+4\sigma_2}+10\mathrm{e}^{6\sigma_1+4\sigma_2}+3\mathrm{e}^{6\sigma_1+6\sigma_2}+(\sigma_1\leftrightarrow\sigma_2)}{(1+\mathrm{e}^{2\sigma_1})^2(1+\mathrm{e}^{2\sigma_2})^2(\mathrm{e}^{2\sigma_1}+\mathrm{e}^{2\sigma_2}+\mathrm{e}^{2\sigma_1+2\sigma_2})^2}\,,\end{aligned} \tag{62}$$

and a very lengthy expression for the one-loop amplitude (see the notebook).

2.3.2. Fermion–gluon states

Next, we address the $\chi_1^3\chi_4$ component and start by exploring its $\mathcal{W}_{[2,2](3,3)}$ contribution. The latter is determined by the gluon–fermion flux-tube excitations created at the bottom and absorbed by the top of the heptagon,

$$\begin{aligned}\mathcal{W}_{[2,2](3,3)}=\mathcal{W}_{\Psi\mathrm{g}|\Psi\mathrm{g}}=\int d\mu_\Psi(u_1)d\mu_{\mathrm{g}}(u_2)\,ix[u_1]\sqrt{x^+[u_2]x^-[u_2]}F_{\Psi\mathrm{g}}(0|u_1,u_2)\\\times P_{\mathrm{g}\Psi|\Psi\mathrm{g}}(-u_2,-u_1|v_2,v_1)\frac{F_{\mathrm{g}\Psi}(-v_1,-v_2|0)}{\sqrt{x^+[v_1]x^-[v_1]}}d\mu_\Psi(v_2)d\mu_{\mathrm{g}}(v_1)\,.\end{aligned} \tag{63}$$

Here the production and annihilation form factors for the flux-tube pair are given in Eqs. (31) and (51), respectively, while the $P_{\mathrm{g}\Psi|\Psi\mathrm{g}}$ is determined by the factorized expression (56). As before, $\mathcal{W}_{\Psi\mathrm{g}|\Psi\mathrm{g}}$ can be decomposed in four terms

$$\mathcal{W}_{\Psi\mathrm{g}|\Psi\mathrm{g}}=\mathcal{W}_{\mathrm{fg}|\mathrm{fg}}+\mathcal{W}_{\mathrm{Fg}|\mathrm{fg}}+\mathcal{W}_{\mathrm{fg}|\mathrm{Fg}}+\mathcal{W}_{\mathrm{Fg}|\mathrm{Fg}}\,, \tag{64}$$

where the first one reads

$$\begin{aligned}\mathcal{W}_{\mathrm{fg}|\mathrm{fg}}=\frac{1}{g^2}\int d\mu_{\mathrm{fg}}(u_2)\sqrt{x^+[u_2]x^-[u_2]}P_{\mathrm{g}|\mathrm{f}}(-u_2|v_1^-)\\\times P_{\mathrm{g}|\mathrm{g}}(-u_2|v_1)P_{\mathrm{f}|\mathrm{f}}(-u_2^-|v_1^-)P_{\mathrm{f}|\mathrm{g}}(-u_2^-|v_1)\frac{x[v_1^-]}{\sqrt{x^+[v_1]x^-[v_1]}}d\mu_{\mathrm{fg}}(v_1)\,.\end{aligned} \tag{65}$$

It accommodates the tree amplitude that reads

$$\begin{aligned}\mathcal{W}^{(0)}_{[2,2](3,3)}=\mathcal{W}^{(0)}_{\mathrm{fg}|\mathrm{fg}}=\pi^2\int\frac{du_2}{2\pi}\frac{dv_1}{2\pi}\frac{\mathrm{e}^{2iu_2\sigma_1+2iv_1\sigma_2}}{\cosh(\pi u_2)\cosh(\pi v_1)}\\\times\frac{(u_2+v_1-i)\Gamma(-iu_2-iv_1)}{(v_1+\frac{i}{2})\Gamma(-\frac{1}{2}-iu_2)\Gamma(-\frac{1}{2}-iv_1)}\end{aligned}$$

$$= -\frac{e^{3\sigma_1+\sigma_2}(e^{2\sigma_1}+e^{2\sigma_2}-e^{2\sigma_1+2\sigma_2}-2e^{4\sigma_1+2\sigma_2})}{(1+e^{2\sigma_1})^2(e^{2\sigma_1}+e^{2\sigma_2}+e^{2\sigma_1+2\sigma_2})^3}\,. \tag{66}$$

A simple counting argument reveals that both $\mathcal{W}_{\mathrm{fg|Fg}}$ and $\mathcal{W}_{\mathrm{Fg|Fg}}$ are of oder $O(g^6)$ and thus start at two-loop order only, while $\mathcal{W}_{\mathrm{Fg|fg}}$ contributes at one-loop already and has to be accounted for. It yields

$$\mathcal{W}^{(1)}_{\mathrm{Fg|fg}} = -i\pi^4 \int \frac{du_1}{2\pi}\frac{du_2}{2\pi}\frac{dv_1}{2\pi}\frac{e^{2i(u_1+u_2)\sigma_1+2iv_1\sigma_2}}{\sinh(\pi u_1)\cosh(\pi u_2)\cosh(\pi v_1)} \times \frac{(u_2+v_1-i)\Gamma(-iu_2-iv_1)\Gamma(\frac{1}{2}-iu_1-iv_1)}{\Gamma(1-iu_1)\Gamma(\frac{3}{2}-iu_2)\Gamma(-\frac{1}{2}-iv_1)\Gamma(\frac{3}{2}-iv_1)}\,, \tag{67}$$

and when added to the one-loop expansion to the $\mathcal{W}_{\mathrm{fg|fg}}$ reproduces the subtracted ratio function

$$\mathcal{W}^{(0)}_{[2,2](3,3)}(\sigma_1,\sigma_2) = \mathcal{P}^{(0)}_{[2,2](3,3)}(\sigma_1,\sigma_2)\,, \tag{68}$$

$$\mathcal{W}^{(1)}_{[2,2](3,3)}(\sigma_1,\sigma_2) = \mathcal{P}^{(1)}_{[2,2](3,3)}(\sigma_1,\sigma_2) + \mathcal{P}^{(0)}_{[1,2](1,3)}(\sigma_1,\sigma_2)r^{(1)}_{1[1]}(\sigma_1) + \mathcal{P}^{(0)}_{[2,1](3,1)}(\sigma_1,\sigma_2)r^{(1)}_{1[1]}(\sigma_2) + \mathcal{P}^{(0)}_{[1,1](1,1)}(\sigma_1,\sigma_2)r^{(1)}_{2[2]}(\sigma_1,\sigma_2)\,. \tag{69}$$

2.3.3. Antifermion–hole states

Let us finally analyze the transition of the antifermion–hole into the fermion–gluon pair. To this end, we consider the $\mathcal{W}_{[2,2](-1,3)}$ contribution to the $\chi_1^3\chi_4$ Grassmann component. Its relation to the ratio function can be found from the general formula (5) and gives to leading and next-to-leading orders

$$\mathcal{W}^{(0)}_{[2,2](-1,3)}(\sigma_1,\sigma_2) = \mathcal{P}^{(0)}_{[2,2](-1,3)}(\sigma_1,\sigma_2)\,, \tag{70}$$

$$\mathcal{W}^{(1)}_{[2,2](-1,3)}(\sigma_1,\sigma_2) = \mathcal{P}^{(1)}_{[2,2](-1,3)}(\sigma_1,\sigma_2) + \mathcal{P}^{(0)}_{[1,2](1,3)}(\sigma_1,\sigma_2)r^{(1)}_{1[1]}(\sigma_1) + \mathcal{P}^{(0)}_{[2,1](-1,1)}(\sigma_1,\sigma_2)r^{(1)}_{1[1]}(\sigma_2)\,. \tag{71}$$

In terms of the flux-tube excitations, $\mathcal{W}_{[2,2](-1,3)}$ can be written as a sum of two contributions

$$\mathcal{W}_{[2,2](-1,3)} = \mathcal{W}_{\bar\Psi\mathrm{h}|\Psi\mathrm{g}} + \mathcal{W}_{\Psi\bar{\mathrm{g}}|\Psi\mathrm{g}}\,. \tag{72}$$

As in several cases analyzed before, only the first term in the sum induces a nonvanishing effects at lowest orders of perturbation theory and takes the form

$$\mathcal{W}_{\bar\Psi\mathrm{h}|\Psi\mathrm{g}} = \int d\mu_\Psi(u_1)d\mu_{\mathrm{h}}(u_2)\frac{ix[u_1]}{g}F^4_{\bar\Psi\mathrm{h}}(0|u_1,u_2) \times \frac{g^2P_{\mathrm{h}\bar\Psi|\Psi\mathrm{g}}(-u_2,-u_1|v_2,v_1)}{x^+[v_1]x^-[v_1]}F_{\mathrm{g}\Psi}(-v_1,-v_2|0)d\mu_{\mathrm{g}}(v_1)d\mu_\Psi(v_2)\,. \tag{73}$$

In fact, out of four contributions spawned by this expression $\mathcal{W}_{\bar\Psi\mathrm{h}|\Psi\mathrm{g}} = \mathcal{W}_{\bar{\mathrm{f}}\mathrm{h}|\mathrm{fg}} + \mathcal{W}_{\bar{\mathrm{F}}\mathrm{h}|\mathrm{fg}} + \mathcal{W}_{\bar{\mathrm{f}}\mathrm{h}|\mathrm{Fg}} + \mathcal{W}_{\bar{\mathrm{F}}\mathrm{h}|\mathrm{Fg}}$, only the one with both fermions belonging to the small fermion sheet accounts for the entire tree and one-loop amplitudes,

$$\mathcal{W}_{\bar{\mathrm{f}}\mathrm{h}|\mathrm{fg}} = \frac{1}{g}\int d\mu_{\mathrm{hf}}(u_2)P_{\mathrm{h}|\mathrm{f}}(-u_2|v_1-\tfrac{i}{2})\frac{P_{\mathrm{h}|\mathrm{g}}(-u_2|v_1)}{\sqrt{x^+[v_1]x^-[v_1]}} \times P_{\bar{\mathrm{f}}|\mathrm{f}}(-u_2+\tfrac{3i}{2}|v_1-\tfrac{i}{2})\frac{P_{\bar{\mathrm{f}}|\mathrm{g}}(-u_2+\frac{3i}{2}|v_1)}{\sqrt{x^+[v_1]x^-[v_1]}}x^-[v_1]d\mu_{\mathrm{gf}}(v_1)\,. \tag{74}$$

Explicitly, it yields the tree level result

$$\mathcal{W}^{(0)}_{\text{fh|fg}} = -i\pi^2 \int \frac{du_2}{2\pi}\frac{dv_1}{2\pi}\frac{e^{2iu_2\sigma_1+2iv_1\sigma_2}}{\cosh(\pi u_2)\cosh(\pi v_1)}\frac{(u_2-\frac{3i}{2})(v_1-\frac{i}{2})\Gamma(1-iu_2-iv_1)}{(v_1+\frac{i}{2})\Gamma(\frac{1}{2}-iu_2)\Gamma(\frac{1}{2}-iv_1)}$$
$$= \frac{e^{5\sigma_1+\sigma_2}(2e^{2\sigma_1}+e^{4\sigma_1}+4e^{2\sigma_2}+5e^{2\sigma_1+2\sigma_2}+e^{4\sigma_1+2\sigma_2})}{(1+e^{2\sigma_1})^2(e^{2\sigma_1}+e^{2\sigma_2}+e^{2\sigma_1+2\sigma_2})^3}\,, \tag{75}$$

with the rest summarized in the accompanying file.

2.4. A glimpse into higher twists: three-particle states

To conclude the discussion of the heptagon, let us take a glance at multiparticle states with twist higher than two. A complete treatment requires analysis of pentagon transitions involving gluonic bound states paired with other flux-tube excitations. Therefore, let us content ourselves with a contribution that is insensitive to these (at least to lowest orders in 't Hooft coupling). We will consider twist-three contribution, i.e., $e^{-3\tau_1-\tau_2}$ to the $\chi_1^3\chi_4$ Grassmann component of the super-Wilson loop. It reads in terms of the corresponding amplitudes

$$\mathcal{W}^{(0)}_{[3,1](-3,1)}(\sigma_1,\sigma_2) = \mathcal{P}^{(0)}_{[3,1](-3,1)}(\sigma_1,\sigma_2)\,, \tag{76}$$
$$\mathcal{W}^{(1)}_{[3,1](-3,1)}(\sigma_1,\sigma_2) = \mathcal{P}^{(1)}_{[3,1](-3,1)}(\sigma_1,\sigma_2) + \mathcal{P}^{(0)}_{[2,1](-1,1)}(\sigma_1,\sigma_2)r^{(1)}_{1[1]}(\sigma_1)$$
$$+ \mathcal{P}^{(0)}_{[1,1](1,1)}(\sigma_1,\sigma_2)r^{(1)}_{1[2]}(\sigma_1)\,, \tag{77}$$

and arises from the production of three antifermion flux-tube excitations in the **4** of SU(4), i.e., $\varepsilon^{ABCD}\bar\psi_B\bar\psi_C\bar\psi_D$ that undergo a transition into a single fermion at the top of the heptagon,

$$\mathcal{W}_{[3,1](-3,1)}(\sigma_1,\sigma_2) = \frac{1}{3!}\int d\mu_\Psi(u_1)d\mu_\Psi(u_2)d\mu_\Psi(u_3)d\mu_\Psi(v_1)x[u_1]x[u_2]x[u_3]x[v_1]$$
$$\times F^{\mathbf{4}}_{\bar\Psi\bar\Psi\bar\Psi}(0|u_1,u_2,u_3)P_{\bar\Psi\bar\Psi\bar\Psi|\Psi}(-u_3,-u_2,-u_1|v_1)\,. \tag{78}$$

Here the form factor for creation of three antifermions as well as the three-to-one pentagon transition both admit factorized forms

$$F^{\mathbf{4}}_{\bar\Psi\bar\Psi\bar\Psi}(0|u_1,u_2,u_3) = \prod_{i<j}^{3}\frac{i}{(u_i-u_j+i)P_{\Psi|\Psi}(u_i|u_j)}\,, \tag{79}$$

$$P_{\bar\Psi\bar\Psi\bar\Psi|\Psi}(-u_3,-u_2,-u_1|v_1) = \frac{\prod_{i=1}^{3}P_{\bar\Psi|\Psi}(-u_i|v_1)}{\prod_{i<j}^{3}P_{\Psi|\Psi}(-u_i|-u_j)} \tag{80}$$

The portion of the integration contour C that belongs to the small fermion sheet induces the leading contribution to the component of the Wilson loops in question. Namely, two out of three antifermions are on the small fermion sheet with the remaining one belongs to the large one. Evaluating the resulting integrals via the Cauchy theorem by picking up the residues in the rational prefactors in the particle creation form factor, we find

$$\mathcal{W}_{[3,1](-3,1)}(\sigma_1,\sigma_2)$$
$$= \frac{1}{2}\int d\mu_{\rm F}(u_1)\mu_{\rm f}(u_1-i)\mu_{\rm f}(u_1-2i)\int d\mu_{\rm F}(v_1)\frac{x[u_1]x[v_1]}{x[u_1-i]x[u_1-2i]}$$
$$\times\frac{P_{\bar{\rm f}|{\rm F}}(-u_1+2i|v_1)P_{\bar{\rm f}|{\rm F}}(-u_1+i|v_1)P_{\bar{\rm F}|{\rm F}}(-u_1|v_1)}{[P_{\bar{\rm f}|{\rm f}}(u_1-2i|u_1-i)]^2_{\pm}[P_{\bar{\rm f}|{\rm F}}(u_1-2i|u_1)]^2_{\pm}[P_{\bar{\rm f}|{\rm F}}(u_1-i|u_1)]^2_{\pm}}\,, \tag{81}$$

where we introduced a shorthand notation $[P_{p_1|p_2}(u_1|u_2)]^2_{\pm} \equiv P_{p_1|p_2}(u_1|u_2)P_{p_1|p_2}(-u_1|-u_2)$. Expanding the integrand to the lowest two orders of perturbation theory, we immediately find an exact agreement with the superloop component $\mathcal{W}_{[3,1](-3,1)}$. For reference, we quote the leading order result

$$\begin{aligned}
&\mathcal{W}^{(0)}_{[3,1](-3,1)}(\sigma_1,\sigma_2)\\
&\quad=-\frac{\pi^2}{2}\int\frac{du_1}{2\pi}\frac{dv_1}{2\pi}\,\frac{e^{2iu_1\sigma_1+2iv_1\sigma_2}}{\sinh(\pi u_1)\sinh(\pi v_1)}\,\frac{(u_1-i)(u_1-2i)\Gamma(1-iu_1-iv_1)}{\Gamma(1-iu_1)\Gamma(1-iv_1)}\\
&\quad=-\frac{(e^{2\sigma_1}+e^{2\sigma_2}+e^{2\sigma_1+2\sigma_2})^3+3e^{2\sigma_1+4\sigma_2}(1+e^{2\sigma_1})(e^{2\sigma_1}+e^{2\sigma_2}+e^{2\sigma_1+2\sigma_2})+e^{6\sigma_1+2\sigma_2}}{(1+e^{2\sigma_1})^3(1+e^{2\sigma_2})(e^{2\sigma_1}+e^{2\sigma_2}+e^{2\sigma_1+2\sigma_2})^3}.
\end{aligned}\tag{82}$$

The one-loop expression is too lengthy to be displayed here and can be found in the companion Mathematica notebook. At two loops and higher, the amplitude receives additive terms from other multiparticle contributions with the same quantum numbers, like two-gluon bound state accompanied by a fermion and two-gluon–fermion states. Their analysis goes beyond the scope of the present work and is deferred to a future publication.

3. Octagon observable

The operator product expansion analysis of the octagon follows the same footsteps. The octagonal super Wilson loop is related in the same fashion to the eight-particle super-ratio function as for the heptagon (5),

$$\mathcal{W}_{8;n}=g^{2n}\mathcal{P}_{8;n}W_8\,,\tag{83}$$

with the only difference that the bosonic loop W_8 receives more terms at each loop order in its perturbative expansion,

$$\begin{aligned}
W_8=1+g^2\Big[&r_1(\tau_1,\sigma_1,\phi_1)+r_1(\tau_2,\sigma_2,\phi_2)+r_1(\tau_3,\sigma_3,\phi_3)\\
&+r_2(\tau_1,\tau_2,\sigma_1,\sigma_2,\phi_1,\phi_2)+r_2(\tau_2,\tau_3,\sigma_2,\sigma_3,\phi_2,\phi_3)\\
&+r_3(\tau_1,\tau_2,\tau_3,\sigma_1,\sigma_2,\sigma_3,\phi_1,\phi_2,\phi_3)\Big]+O(g^4)\,.
\end{aligned}\tag{84}$$

While the functions r_1 and r_2 are the same as in Section 2 and were determined earlier in Eqs. (8) and (12), respectively, the new ingredient r_3 depends on all three triplets of conformal cross ratios (see Appendix A) and reads to leading order in the OPE

$$\begin{aligned}
r_3(\tau_1,\tau_2,\tau_3,\sigma_1,\sigma_2,\sigma_3,\phi_1,\phi_2,\phi_3)=e^{-\tau_1-\tau_2-\tau_3}&(e^{i\phi_1+i\phi_2+i\phi_3}\\
&+e^{-i\phi_1-i\phi_2-i\phi_3})r_{3[3]}(\sigma_1,\sigma_2,\sigma_3)+\dots\,,
\end{aligned}\tag{85}$$

where the σ-dependent coefficient is represented by a consecutive sequence of gluonic pentagon transitions

$$r_{3[3]}(\sigma_1,\sigma_2,\sigma_3)=\frac{1}{g^2}\int d\mu_g(u)P_{g|g}(-u|v)d\mu_g(v)P_{g|g}(-v|w)d\mu_g(w)\,.\tag{86}$$

The helicity-violating contribution sets in starting from two loops [14] and is thus irrelevant for our present discussion.

Due to a plethora of various contributions to the octagon OPE, let us discuss a few illustrative examples. The NMHV octagon admits the following Grassmann decomposition

$$\begin{aligned}\mathcal{W}_{8;1} = \chi_1^2\chi_4^2\Big\{&\mathrm{e}^{-\tau_1-\tau_2-\tau_3}\mathcal{W}_{[1,1,1](0,0,0)}\\ &+\mathrm{e}^{-2\tau_1-\tau_2-\tau_3}\mathrm{e}^{-i\phi_1}\mathcal{W}_{[2,1,1](-2,0,0)}+\mathrm{e}^{-\tau_1-2\tau_2-\tau_3}\mathrm{e}^{-i\phi_2}\mathcal{W}_{[1,2,1](0,-2,0)}+\dots\Big\}\\ &+\chi_1^3\chi_4\Big\{\mathrm{e}^{-\tau_1-\tau_2-\tau_3}\mathrm{e}^{i\phi_1/2+i\phi_2/2+i\phi_3/2}\mathcal{W}_{[1,1,1](1,1,1)}\\ &+\mathrm{e}^{-2\tau_1-\tau_2-\tau_3}\Big[\mathrm{e}^{3i\phi_1/2+i\phi_2/2+i\phi_3/2}\mathcal{W}_{[2,1,1](3,1,1)}\\ &+\mathrm{e}^{-i\phi_1/2+i\phi_2/2+i\phi_3/2}\mathcal{W}_{[2,1,1](-1,1,1)}\Big]+\dots\Big\}\\ &+\dots\,.\end{aligned} \tag{87}$$

Below, we will provide in turn the flux-tube interpretation for corresponding coefficients to all orders in coupling and test them against available perturbative data [35].

3.1. Single-particle states

The leading twist contributions to the components in question are

$$\mathcal{W}_{[1,1,1](0,0,0)} = -\int d\mu_{\mathrm{h}}(u)P_{\mathrm{h}|\mathrm{h}}(-u|v)d\mu_{\mathrm{h}}(v)P_{\mathrm{h}|\mathrm{h}}(-v|w)d\mu_{\mathrm{h}}(w)\,, \tag{88}$$

$$\mathcal{W}_{[1,1,1](1,1,1)} = -i\int d\mu_{\Psi}(u)x[u]\,P_{\Psi|\Psi}(-u|v)d\mu_{\Psi}(v)P_{\Psi|\Psi}(-v|w)d\mu_{\Psi}(w)\,. \tag{89}$$

The first equation here was already discussed in Ref. [14]. In the second one, only the branch of the fermion on the large Riemann sheet induces a nonvanishing effect in weak coupling expansion, i.e., $\Psi = \mathrm{F}$. At leading order, these read

$$\mathcal{W}^{(0)}_{[1,1,1](0,0,0)} = \frac{-\mathrm{e}^{\sigma_1+\sigma_2+\sigma_3}}{\mathrm{e}^{2\sigma_2}+\mathrm{e}^{2\sigma_1+2\sigma_2}+\mathrm{e}^{2\sigma_1+2\sigma_3}+\mathrm{e}^{2\sigma_2+2\sigma_3}+\mathrm{e}^{2\sigma_1+2\sigma_2+2\sigma_3}}\,, \tag{90}$$

$$\mathcal{W}^{(0)}_{[1,1,1](1,1,1)} = \frac{\mathrm{e}^{2\sigma_1+2\sigma_3}}{(1+\mathrm{e}^{2\sigma_1})(\mathrm{e}^{2\sigma_2}+\mathrm{e}^{2\sigma_1+2\sigma_2}+\mathrm{e}^{2\sigma_1+2\sigma_3}+\mathrm{e}^{2\sigma_2+2\sigma_3}+\mathrm{e}^{2\sigma_1+2\sigma_2+2\sigma_3})}\,. \tag{91}$$

Together with subleading corrections in g^2, calculated with expressions provided in Appendix B, they agree with the one-loop ratio function (see the attached file).

3.2. Two-particle states

Let us analyze now twist-two contributions.

3.2.1. Two-(anti)fermion states

Starting with $\mathcal{W}_{[2,1,1](-2,0,0)}$, the latter is determined by the sum of two twist-two components created at the bottom of the loop, $\mathcal{W}_{[2,1,1](-2,0,0)} = \mathcal{W}_{\bar{\Psi}\bar{\Psi}|\mathrm{h}|\mathrm{h}} + \mathcal{W}_{\bar{\mathrm{g}}\mathrm{h}|\mathrm{h}|\mathrm{h}}$. However, as in the case of the heptagon discussed at the end of Section 2.2.1, only the first one induces the leading two orders of perturbation theory,

$$\mathcal{W}_{\bar\Psi\bar\Psi|\mathrm{h}|\mathrm{h}} = \frac{1}{g^2}\int d\mu_\Psi(u_1) d\mu_\Psi(u_2) F^{\mathbf{6}}_{\Psi\Psi}(0|u_1,u_2) P_{\bar\Psi\bar\Psi|\mathrm{h}}(-u_2,-u_1|v_1) \times d\mu_{\mathrm{h}}(v_1) P_{\mathrm{h}|\mathrm{h}}(-v_1|w_1) d\mu_{\mathrm{h}}(w_1)\,, \tag{92}$$

in particular, in the kinematics when one of the antifermions in the pair belongs to the small sheet while the other one to the large one,

$$\mathcal{W}_{\bar{\mathrm{f}}\mathrm{F}|\mathrm{h}|\mathrm{h}} = \frac{1}{g^2}\int d\mu_{\mathrm{fF}}(u_2) \frac{x[u_2-i]}{x[u_2]} P_{\bar{\mathrm{f}}|\mathrm{h}}(-u_2+i|v_1) P_{\mathrm{F}|\mathrm{h}}(-u_2|v_1) d\mu_{\mathrm{h}}(v_1) \times P_{\mathrm{h}|\mathrm{h}}(-v_1|w_1) d\mu_{\mathrm{h}}(w_1)\,. \tag{93}$$

At leading order, we obtain

$$\begin{aligned}
&\mathcal{W}^{(0)}_{\mathrm{fF}|\mathrm{h}|\mathrm{h}} \\
&= \pi^3 \int \frac{du_2}{2\pi}\frac{dv_1}{2\pi}\frac{dw_1}{2\pi} \frac{\mathrm{e}^{2iu_2\sigma_1+2iv_1\sigma_2+2iw_1\sigma_3}}{\sinh(\pi u_2)\cosh(\pi v_1)\cosh(\pi w_1)} \\
&\quad\times \frac{(u_2-i)\Gamma(\frac12-iu_2-iv_1)\Gamma(-iv_1-iw_1)}{\Gamma(1-iu_2)\Gamma^2(\frac12-iv_1)\Gamma(\frac12-iw_1)} \\
&= -\frac{\mathrm{e}^{5\sigma_2+\sigma_3}(1+\mathrm{e}^{2\sigma_3})^2}{(\mathrm{e}^{2\sigma_2}+\mathrm{e}^{2\sigma_3}+\mathrm{e}^{2\sigma_2+2\sigma_3})(\mathrm{e}^{2\sigma_2}+\mathrm{e}^{2\sigma_1+2\sigma_2}+\mathrm{e}^{2\sigma_1+2\sigma_3}+\mathrm{e}^{2\sigma_2+2\sigma_3}+\mathrm{e}^{2\sigma_1+2\sigma_2+2\sigma_3})^2}\,.
\end{aligned} \tag{94}$$

It agrees with the corresponding ratio function $\mathcal{P}^{(0)}_{[2,1,1](-2,0,0)}$ along with its first subleading term $\mathcal{P}^{(1)}_{[2,1,1](-2,0,0)}$,

$$\mathcal{W}^{(0)}_{[2,1,1](-2,0,0)}(\sigma_1,\sigma_2,\sigma_3) = \mathcal{P}^{(0)}_{[2,1,1](-2,0,0)}(\sigma_1,\sigma_2,\sigma_3)\,, \tag{95}$$

$$\mathcal{W}^{(1)}_{[2,1,1](-2,0,0)}(\sigma_1,\sigma_2,\sigma_3) = \mathcal{P}^{(1)}_{[2,1,1](-2,0,0)}(\sigma_1,\sigma_2,\sigma_3) + \mathcal{P}^{(0)}_{[1,1,1](0,0,0)}(\sigma_1,\sigma_2,\sigma_3) r^{(1)}_{1[1]}(\sigma_1)\,, \tag{96}$$

as shown in the notebook.

3.2.2. Antifermion–hole states

Turning to the $\chi_1^3\chi_4$ component, we consider the antifermion–hole state first. It follows the analysis in Section 2.2.2, so we will be brief here. As for the heptagon, the lowest two orders in perturbation theory for $\mathcal{W}_{[2,1,1](-1,1,1)}$ are governed by the antifermion–hole pair in the initial state $\mathcal{W}_{\bar\Psi\mathrm{h}|\Psi|\Psi}$, i.e., $\mathcal{W}_{[2,1,1](-1,1,1)} = \mathcal{W}_{\bar\Psi\mathrm{h}|\Psi|\Psi} + O(g^6)$, where

$$\mathcal{W}_{\bar\Psi\mathrm{h}|\Psi} = \int d\mu_\Psi(u_1)\, d\mu_{\mathrm{h}}(u_2)\, \frac{ix[u_1]}{g^2} F^{\mathbf{4}}_{\bar\Psi\mathrm{h}}(0|u_1,u_2) \times P_{\mathrm{h}\bar\Psi|\Psi}(-u_2,-u_1|v_1)\, d\mu_\Psi(v_1) P_{\Psi|\Psi}(-v_1|w_1)\, d\mu_\Psi(w_1)\,, \tag{97}$$

and more precisely by the contribution from the small fermion sheet in the initial state

$$\mathcal{W}_{\bar{\mathrm{f}}\mathrm{h}|\mathrm{F}|\mathrm{F}} = \frac{1}{g}\int d\mu_{\mathrm{f}\mathrm{h}}(u_2) P_{\bar{\mathrm{f}}|\mathrm{F}}(-u_2+\tfrac{3i}{2}|v_1) P_{\mathrm{h}|\mathrm{F}}(-u_2|v_1) d\mu_{\mathrm{F}}(v_1) \times P_{\mathrm{F}|\mathrm{F}}(-v_1|w_1) d\mu_{\mathrm{F}}(w_1)\,. \tag{98}$$

Employing its perturbative expansion summarized in Appendix B, we find

$$
\begin{aligned}
&\mathcal{W}^{(0)}_{[2,1,1](-1,1,1)}\\
&\quad= i\pi^3\int\frac{du_2}{2\pi}\frac{dv_1}{2\pi}\frac{dw_1}{2\pi}\frac{\mathrm{e}^{2iu_2\sigma_1+2iv_1\sigma_2+2iw_1\sigma_3}}{\cosh(\pi u_2)\sinh(\pi v_1)\sinh(\pi w_1)}\\
&\qquad\times\frac{(u_2-\frac{3i}{2})\Gamma(\frac12-iu_2-iv_1)\Gamma(-iv_1-iw_1)}{\Gamma(\frac12-iu_2)\Gamma(1-iv_1)\Gamma(-iv_1)\Gamma(1-iw_1)}\\
&\quad=\frac{\mathrm{e}^{3\sigma_1+2\sigma_3}(3+\mathrm{e}^{2\sigma_1})(\mathrm{e}^{2\sigma_2}+\mathrm{e}^{2\sigma_1+2\sigma_2}+\mathrm{e}^{2\sigma_1+2\sigma_3}+\mathrm{e}^{2\sigma_2+2\sigma_3}+\mathrm{e}^{2\sigma_1+2\sigma_2+2\sigma_3})-\mathrm{e}^{5\sigma_1+4\sigma_3}}{(1+\mathrm{e}^{2\sigma_1})^2(\mathrm{e}^{2\sigma_2}+\mathrm{e}^{2\sigma_1+2\sigma_2}+\mathrm{e}^{2\sigma_1+2\sigma_3}+\mathrm{e}^{2\sigma_2+2\sigma_3}+\mathrm{e}^{2\sigma_1+2\sigma_2+2\sigma_3})^2}.
\end{aligned}
\tag{99}
$$

The agreement persists for $\mathcal{W}^{(1)}_{[2,1,1](-1,1,1)}$ at one loop order (see the ancillary file) with the subtracted ratio function defined by Eq. (96), where one obviously has to replace the helicity subscripts as follows $(-2,0,0)\to(-1,1,1)$.

3.2.3. Fermion–gluon states

We finish the analysis of the $\chi_1^3\chi_4$ component by unraveling the structure of its $\mathcal{W}_{[2,1](3,1)}$ term. The tree and one-loop coefficients in the perturbative expansion of the latter are related to the ratio function via the relations (95) and (96), where the weight $(2,0,0)$ gets substituted by $(3,1,1)$. The analysis of quantum numbers suggests that this component is induced by the emission of the gluon–fermion pair at the bottom of the hexagon and absorption of a single fermion at the top. Thus its all-order expression reads

$$
\begin{aligned}
\mathcal{W}_{[2,1,1](3,1,1)}=\mathcal{W}_{\Psi g|\Psi|\Psi}=\int d\mu_\Psi(u_1)\,d\mu_g(u_2)\,ix[u_1]\,\frac{\sqrt{x^+[u_2]x^-[u_2]}}{g}\\
\times F_{\Psi g}(0|u_1,u_2)P_{g\Psi|\Psi}(-u_2,-u_1|v_1)\,d\mu_\Psi(v_1)\\
\times P_{\Psi|\Psi}(-v_1|w_1)\,d\mu_\Psi(w_1)\,.
\end{aligned}
\tag{100}
$$

The leading effects arise from the small fermion in the incoming state

$$
\begin{aligned}
\mathcal{W}_{fg|F|F}=\frac1g\int d\mu_{fg}(u_2)\,\sqrt{x^+[u_2]x^-[u_2]}P_{f|F}(-u_2+\tfrac{i}{2}|v_1)P_{g|F}(-u_2|v_1)d\mu_F(v_1)\\
\times P_{F|F}(-v_1|w_1)d\mu_F(w_1)\,.
\end{aligned}
\tag{101}
$$

The ratio function $\mathcal{W}_{[2,1,1](3,1,1)}$ with the leading term yielding explicitly

$$
\begin{aligned}
&\mathcal{W}^{(0)}_{[2,1,1](3,1,1)}\\
&\quad=\pi^3\int\frac{du_2}{2\pi}\frac{dv_1}{2\pi}\frac{dw_1}{2\pi}\frac{\mathrm{e}^{2iu_2\sigma_1+2iv_1\sigma_2+2iw_1\sigma_3}}{\cosh(\pi u_2)\sinh(\pi v_1)\sinh(\pi w_1)}\\
&\qquad\times\frac{\Gamma(\frac12-iu_2-iv_1)\Gamma(-v_1-iw_1)}{\Gamma(-\frac12-iu_2)\Gamma(1-iv_1)\Gamma(-iv_1)\Gamma(1-iw_1)}\\
&\quad=\frac{\mathrm{e}^{3\sigma_1+2\sigma_3}(2\mathrm{e}^{2\sigma_2}+2\mathrm{e}^{2\sigma_1+2\sigma_2}+\mathrm{e}^{2\sigma_1+2\sigma_3}+2\mathrm{e}^{2\sigma_2+2\sigma_3}+2\mathrm{e}^{2\sigma_1+2\sigma_2+2\sigma_3})}{(1+\mathrm{e}^{2\sigma_1})^2(\mathrm{e}^{2\sigma_2}+\mathrm{e}^{2\sigma_1+2\sigma_2}+\mathrm{e}^{2\sigma_1+2\sigma_3}+\mathrm{e}^{2\sigma_2+2\sigma_3}+\mathrm{e}^{2\sigma_1+2\sigma_2+2\sigma_3})^2}\,.
\end{aligned}
\tag{102}
$$

The next-to-leading order in 't Hooft coupling for the ratio function coincides with the OPE prediction as well.

4. Conclusions

In this paper, we constructed the OPE for higher polygons (heptagons and octagons) within the integrability-based pentagon approach. We considered the Grassmann degree-four components of the null polygonal Wilson loops which are dual to NMHV ratio function in maximally supersymmetric Yang–Mills theory. The goal of this consideration was twofold. First, we tested the factorization hypothesis for multiparticle transitions in terms of single-particle ones which is rooted in the integrability of the flux-tube dynamics. Currently, the fact that the bootstrap equations obeyed by fermionic excitations are nonlinear in nature obscures the derivation of the factorized form for these transitions. Second, we verified the correctness of the charged single-particle pentagons derived from a set of postulated axioms in previous studies. Explicit perturbative data on scattering amplitudes involving more than six particles is rather scarce. Currently, the only available source for an arbitrary number of legs is the one-loop calculation of Ref. [35] cast in the form of a Mathematica routine. Making heavy use of the latter, both items on our agenda received positive confirmation. We observed that in all cases considered, two-particle contributions involving at least one fermion induced tree-level amplitudes when the latter belonged to the small-fermion sheet thus acting as a supersymmetry transformation on the accompanying flux-tube excitation. Compared to the previously analyzed NMHV hexagon, for higher polygons the onset of genuine two-particle states was lowered from two- to one-loop order exhibiting their stronger sensitivity to higher twist components of the flux-tube wave functions.

Having tested all charged pentagons, one can immediately generate results at any order of perturbation theory (or at finite coupling). A natural next step is to analyze the behavior of various components at strong coupling. Also there is no difficulty of principle to consider even higher polygons as well as any helicity configurations of incoming particles at higher twists. Currently, the only missing blocks on the way of achieving this for all possible components, are the charged pentagons involving the gauge field bound states undergoing transitions into other flux-tube excitations. This question is currently under study and results will be discussed elsewhere.

Acknowledgements

We are grateful to Jacob Bourjaily, Lance Dixon and Jaroslav Trnka for instructive discussions and correspondence. We would like to thank Benjamin Basso for informing us about a forthcoming work [30] where similar questions are addressed. This work was supported by the U.S. National Science Foundation under the grants PHY-1068286 and PHY-1403891.

Appendix A. Reference polygons

In this appendix we will outline a recursive construction of reference polygons which are used in the main body of the paper. We start from a reference square shown in (leftmost panel in) Fig. 2 that is defined by [14]

$$Z_1^{(4)} = (0,0,1,0)\,, \qquad Z_2^{(4)} = (1,0,0,0)\,,$$
$$Z_3^{(4)} = (0,0,0,1)\,, \qquad Z_4^{(4)} = (0,1,0,0)\,. \tag{A.1}$$

The latter is invariant under the conformal transformation

$$Z_j^{(4)} = Z_j^{(4)} \cdot M(\tau,\sigma,\phi) \tag{A.2}$$

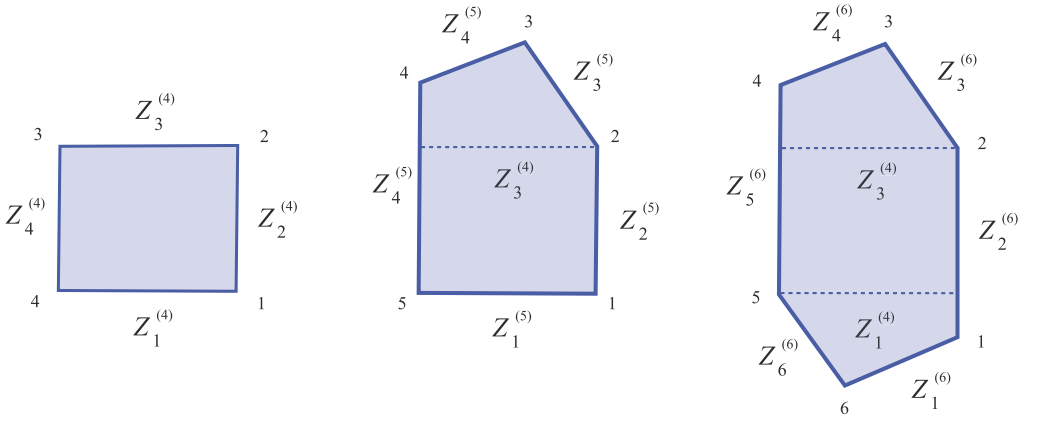

Fig. 2. Recursive construction of reference pentagons and hexagons from a square.

where the equality sign stands for "equal up to rescaling", with

$$M(\tau,\sigma,\phi)=\begin{pmatrix} e^{\sigma-i\phi/2} & & & \\ & e^{-\sigma-i\phi/2} & & \\ & & e^{\tau+i\phi/2} & \\ & & & e^{-\tau+i\phi/2} \end{pmatrix}. \tag{A.3}$$

This matrix parametrizes the three conformal symmetries of the square that play a crucial role in the OPE framework [2].

Adding two more twistor lines on top of the square as shown by the middle graph in Fig. 2, one can construct a reference pentagon. As one can see, three out of five sides of the latter coincide with the square

$$Z_1^{(5)}=Z_1^{(4)}\,,\qquad Z_2^{(5)}=Z_2^{(4)}\,,\qquad Z_5^{(5)}=Z_4^{(4)}\,. \tag{A.4}$$

While the components of the remaining two, $Z_3^{(5)}$ and $Z_4^{(5)}$, are determined by the intersection and space-like interval conditions. Namely, the condition of intersection of three twistor lines in the same point X_2,

$$X_2\equiv Z_2^{(4)}\wedge Z_3^{(4)}=Z_2^{(4)}\wedge Z_3^{(5)}=Z_3^{(4)}\wedge Z_3^{(5)} \tag{A.5}$$

uniquely fixes $Z_3^{(5)}$ to be

$$Z_3^{(5)}=(-1,0,0,1)\,. \tag{A.6}$$

The space-like nature of the intervals $(X_{13}^{(5)})^2$, $(X_{24}^{(5)})^2$ and $(X_{35}^{(5)})^2$, allows one to find (up to an overall scale) the last twistor

$$Z_4^{(5)}=(0,1,-1,1)\,. \tag{A.7}$$

Higher polygons are constructed accordingly by successively extending either the bottom or the top portions of the preceding polygons. The hexagon is demonstrated in the leftmost panel of Fig. 2 is encoded by the following twistors

$$Z_1^{(6)}=(1,0,1,1)\,,\qquad Z_2^{(6)}=(1,0,0,0)\,,\qquad Z_3^{(6)}=(-1,0,0,1)\,, \tag{A.8}$$

$$Z_4^{(6)}=(0,1,-1,1)\,,\qquad Z_5^{(6)}=(0,1,0,0)\,,\qquad Z_6^{(6)}=(0,1,1,0)\,. \tag{A.9}$$

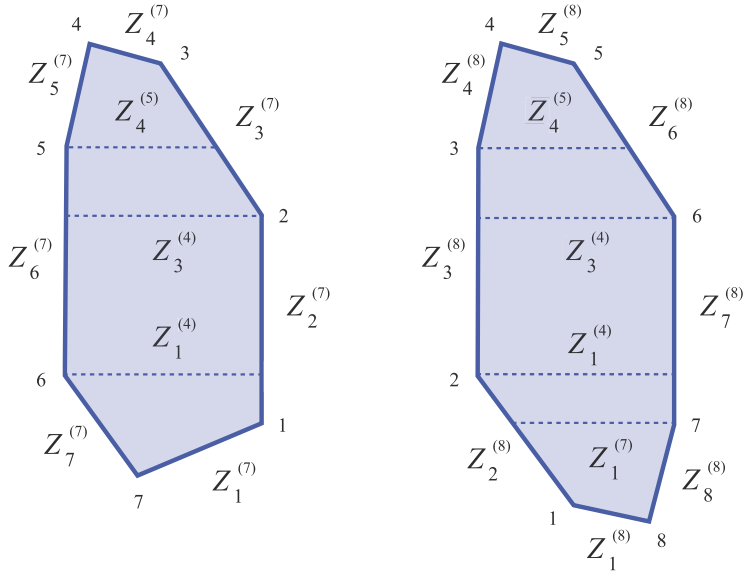

Fig. 3. Tessellation of heptagons and octagons.

The heptagon and octagon are displayed in Fig. 3. Noticed that we flipped the assignment of twistors for the octagon to have all polygons parametrized in the same fashion. The corresponding reference twistors are

$$
\begin{aligned}
&Z_1^{(7)} = (1,0,1,1)\,, \qquad Z_2^{(7)} = (1,0,0,0)\,, \qquad Z_3^{(7)} = (-1,0,0,1)\,,\\
&Z_4^{(7)} = (-1,1,-1,3)\,, \qquad Z_5^{(7)} = (0,2,-1,1)\,, \qquad Z_6^{(7)} = (0,1,0,0)\,,\\
&Z_7^{(7)} = (0,1,1,0)\,,
\end{aligned}
\tag{A.10}
$$

and

$$
\begin{aligned}
&Z_1^{(8)} = (1,1,3,1)\,, \qquad Z_2^{(8)} = (0,1,1,0)\,, \qquad Z_3^{(8)} = (0,1,0,0)\,,\\
&Z_4^{(8)} = (0,2,-1,1)\,, \qquad Z_5^{(8)} = (-1,1,-1,3)\,, \qquad Z_6^{(8)} = (-1,0,0,1)\,,\\
&Z_7^{(8)} = (1,0,0,0)\,, \qquad Z_8^{(8)} = (2,0,1,1)\,,
\end{aligned}
\tag{A.11}
$$

respectively.

Notice that this construction provides a natural tessellation of null polygons: they are divided in a series of pentagon transitions that overlap on intermediate null squares. To encode all inequivalent polygons we will apply conformal symmetries of these middle squares on all twistors above or below them. All hexagons are then defined by the set

$$
\mathbf{Z}^{(6)} = \{Z_1^{(6)} \cdot M(\tau,\sigma,\phi)\,,\ Z_2^{(6)}\,,\ Z_3^{(6)}\,,\ Z_4^{(6)}\,,\ Z_5^{(6)}\,,\ Z_6^{(6)} \cdot M(\tau,\sigma,\phi)\}\,. \tag{A.12}
$$

To define heptagons, while the bottom middle square is invariant under the same transformation M as defined in Eq. (A.3), the top middle square is conformally invariant with respect to the matrix multiplication with

$$M'(\tau,\sigma,\phi)=\begin{pmatrix} e^{-\sigma-i\phi/2} & & & -e^{-\sigma-i\phi/2}+e^{\tau+i\phi/2} \\ & e^{\sigma-i\phi/2} & & \\ & e^{\sigma-i\phi/2}-e^{-\tau+i\phi/2} \quad e^{-\tau+i\phi/2} & e^{\tau+i\phi/2}-e^{-\tau+i\phi/2} & \\ & & & e^{\tau+i\phi/2} \end{pmatrix}. \tag{A.13}$$

Then all heptagons are parametrized by the set of twistors

$$\begin{aligned} \boldsymbol{Z}^{(7)}=\{&Z_1^{(7)}\cdot M(\tau_1,\sigma_1,\phi_1),\ Z_2^{(7)},\ Z_3^{(7)},\ Z_4^{(7)}\cdot[M'(\tau_2,\sigma_2,\phi_2)]^{-1},\\ &Z_5^{(7)}\cdot[M'(\tau_2,\sigma_2,\phi_2)]^{-1},\ Z_6^{(7)},\ Z_7^{(7)}\cdot M(\tau_1,\sigma_1,\phi_1)\}. \end{aligned} \tag{A.14}$$

To define the octagons, we have to find the symmetries of the bottom middle square. The latter is invariant with respect to the transformation matrix

$$M''(\tau,\sigma,\phi)=\begin{pmatrix} e^{-\sigma-i\phi/2} & & & \\ & e^{\sigma-i\phi/2} & e^{\sigma-i\phi/2}-e^{-\tau+i\phi/2} & \\ & & e^{-\tau+i\phi/2} & \\ -e^{-\sigma-i\phi/2}+e^{\tau+i\phi/2} & & e^{\tau+i\phi/2}-e^{-\tau+i\phi/2} & e^{\tau+i\phi/2} \end{pmatrix}, \tag{A.15}$$

such that the momentum twistors parametrizing all inequivalent octagons read

$$\begin{aligned} \boldsymbol{Z}^{(8)}=\{&Z_1^{(8)}\cdot M''(\tau_1,\sigma_1,\phi_1)\cdot M(\tau_2,\sigma_2,\phi_2),\ Z_2^{(8)}\cdot M(\tau_2,\sigma_2,\phi_2),\ Z_3^{(8)},\\ &Z_4^{(8)}\cdot[M'(\tau_3,\sigma_3,\phi_3)]^{-1},\ Z_5^{(8)}\cdot[M'(\tau_3,\sigma_3,\phi_3)]^{-1},\ Z_6^{(8)},\ Z_7^{(8)},\\ &Z_8^{(8)}\cdot M''(\tau_1,\sigma_1,\phi_1)\cdot M(\tau_2,\sigma_2,\phi_2)\}. \end{aligned} \tag{A.16}$$

Appendix B. Pentagons, measures, energies and momenta

In this appendix, we summarize pentagon transitions for all single flux-tube excitations to one loop order. These obey the property

$$P_{p_1|p_2}(u_1|u_2)=P_{p_2|\bar{p}_1}(-u_2|-u_1). \tag{B.17}$$

To simplify notations, we use the harmonic numbers of degree r, $H_u^{(r)}$ instead of Euler polygamma functions. We list below the boson–boson, boson–fermion and fermion–fermion transitions, respectively.

Boson–boson pentagons [14,16]:

$$\begin{aligned} P_{h|h}(u|v)=&\frac{\Gamma(iu-iv)}{g^2\,\Gamma(\frac12+iu)\Gamma(\frac12-iv)}\\ &+\frac{\Gamma(iu-iv)}{\Gamma(\frac12+iu)\Gamma(\frac12-iv)}\Big[H_{-1/2+iu}H_{-1/2+iv}+H_{-1/2-iu}H_{-1/2+iv}\\ &-H_{-1/2+iu}H_{-1/2-iv}+H_{-1/2-iu}H_{-1/2-iv}-H^{(2)}_{-1/2+iu}-H^{(2)}_{-1/2-iv}\Big]\\ &+O(g^2), \end{aligned} \tag{B.18}$$

$$P_{h|g}(u|v)=\frac{\Gamma(1+iu-iv)}{g\,\Gamma(\frac12+iu)\Gamma(\frac12-iv)}\sqrt{\frac{v^-}{v^+}}$$

$$
\begin{aligned}
&+\frac{g\Gamma(1+iu-iv)}{\Gamma(\frac{1}{2}+iu)\Gamma(\frac{1}{2}-iv)}\sqrt{\frac{v^-}{v^+}}\Big[H_{-1/2+iu}H_{-1/2+iv}+H_{-1/2-iu}H_{1/2+iv}\\
&-H_{-1/2+iu}H_{-1/2-iv}+H_{-1/2-iu}H_{1/2-iv}-H^{(2)}_{-1/2+iu}-H^{(2)}_{-1/2-iv}\\
&-\frac{iv}{(v^+v^-)^2}\Big]+O(g^3)\,, \qquad \text{(B.19)}\\
P_{\mathrm{g|g}}(u|v)=&-\frac{\Gamma(iu-iv)}{g^2\Gamma(-\frac{1}{2}+iu)\Gamma(-\frac{1}{2}-iv)}\\
&-\frac{\Gamma(iu-iv)}{2\Gamma(-\frac{1}{2}+iu)\Gamma(-\frac{1}{2}-iv)}\Big[8\zeta_2+\frac{1-4u^2}{2(u^+u^-)^2}+\frac{1}{(v^+v^-)^2}\\
&-\frac{1+4u^2+8uv}{2u^+u^-v^+v^-}\\
&+\big(H_{1/2-iu}+H_{1/2+iu}-i\pi\tanh(\pi u)\big)\big(H_{1/2-iv}+H_{1/2+iv}+i\pi\tanh(\pi v)\big)\\
&+H^{(2)}_{1/2-iu}-H^{(2)}_{1/2+iu}-H^{(2)}_{1/2-iv}+H^{(2)}_{1/2+iv}-\pi^2\tanh^2(\pi u)-\pi^2\tanh^2(\pi v)\\
&-2\pi^2\tanh(\pi u)\tanh(\pi v)\Big]+O(g^2)\,, \qquad \text{(B.20)}\\
P_{\bar{\mathrm{g}}|\mathrm{g}}(u|v)=&\frac{\Gamma(2+iu-iv)}{\Gamma(\frac{3}{2}+iu)\Gamma(\frac{3}{2}-iv)}\\
&+\frac{g^2\Gamma(2+iu-iv)}{2\Gamma(\frac{3}{2}+iu)\Gamma(\frac{3}{2}-iv)}\Big[8\zeta_2-\frac{1-4u^2}{2(u^+u^-)^2}-\frac{1}{(v^+v^-)^2}+\frac{1+4u^2+8uv}{2u^+u^-v^+v^-}\\
&+\big(H_{1/2-iu}+H_{1/2+iu}-i\pi\tanh(\pi u)\big)\big(H_{1/2-iv}+H_{1/2+iv}+i\pi\tanh(\pi v)\big)\\
&+H^{(2)}_{1/2-iu}-H^{(2)}_{1/2+iu}-H^{(2)}_{1/2-iv}+H^{(2)}_{1/2+iv}-\pi^2\tanh^2(\pi u)-\pi^2\tanh^2(\pi v)\\
&-2\pi^2\tanh(\pi u)\tanh(\pi v)\Big]+O(g^4)\,. \qquad \text{(B.21)}
\end{aligned}
$$

Boson–fermion pentagons [18]:

$$
\begin{aligned}
P_{\mathrm{h|F}}(u|v)=&\frac{v\Gamma(\frac{1}{2}+iu-iv)}{g\Gamma(\frac{1}{2}+iu)\Gamma(1-iv)}\\
&+\frac{g\,v\Gamma(\frac{1}{2}+iu-iv)}{\Gamma(\frac{1}{2}+iu)\Gamma(1-iv)}\Big[H_{-1/2-iu}H_{-iv}-H_{-1/2+iu}H_{-1-iv}\\
&+H_{-1/2-iu}H_{iv}+H_{-1/2+iu}H_{iv}-H^{(2)}_{-1/2+iu}-H^{(2)}_{-1-iv}\Big]+O(g^4)\,, \qquad \text{(B.22)}\\
P_{\mathrm{h|f}}(u|v)=&\frac{g}{v}+\frac{g^3}{v^3}\big(1-ivH_{-1/2+iu}\big)+O(g^4)\,, \qquad \text{(B.23)}\\
P_{\mathrm{g|F}}(u|v)=&\frac{v\Gamma(\frac{1}{2}+iu-iv)}{g\,\Gamma(\frac{1}{2}+iu)\Gamma(1-iv)}\sqrt{\frac{u^+}{u^-}}\\
&+\frac{g\,v\Gamma(\frac{1}{2}+iu-iv)}{\Gamma(\frac{1}{2}+iu)\Gamma(1-iv)}\sqrt{\frac{u^+}{u^-}}\Big[\frac{iu}{(u^+u^-)^2}+H_{1/2+iu}H_{iv}+H_{1/2-iu}H_{-1+iv}
\end{aligned}
$$

$$- H_{-1/2+iu}H_{-1-iv} + H_{-1/2-iu}H_{-1-iv} - H^{(2)}_{-1/2+iu} - H^{(2)}_{-1-iv}\Big] + O(g^3)\,, \tag{B.24}$$

$$P_{\mathrm{g}|\mathrm{f}}(u|v) = \frac{ig(u-v+\frac{i}{2})}{v\sqrt{x^+[u]x^-[u]}}\left\{1+\frac{g^2}{v}\left[\frac{1}{v} - iH_{-3/2+iu}\right]\right\} + O(g^5)\,,$$

$$P_{\bar{\mathrm{g}}|\mathrm{F}}(u|v) = \frac{\Gamma(\frac{3}{2}+iu-iv)}{g\,\Gamma(\frac{1}{2}+iu)\Gamma(1-iv)}\sqrt{\frac{u^+}{u^-}}$$
$$+ \frac{g\Gamma(\frac{3}{2}+iu-iv)}{\Gamma(\frac{1}{2}+iu)\Gamma(1-iv)}\sqrt{\frac{u^+}{u^-}}\Big[\frac{iu}{(u^+u^-)^2} + H_{1/2+iu}H_{-1+iv} - H_{-1/2+iu}H_{-iv}$$
$$+ H_{1/2-iu}H_{iv} + H_{-1/2-iu}H_{-iv} - H^{(2)}_{-1/2+iu} - H^{(2)}_{-iv}\Big] + O(g^3)\,, \tag{B.25}$$

$$P_{\bar{\mathrm{g}}|\mathrm{f}}(u|v) = \frac{i}{g}\sqrt{x^+[u]x^-[u]}\left\{1 - \frac{ig^2}{v}H_{1/2+iu} + O(g^4)\right\}. \tag{B.26}$$

Fermion–fermion pentagons [15]:

$$P_{\mathrm{F}|\mathrm{F}}(u|v) = \frac{\Gamma(iu-iv)}{g^2\Gamma(iu)\Gamma(-iv)}$$
$$+ \frac{\Gamma(iu-iv)}{\Gamma(iu)\Gamma(-iv)}\Big[-\frac{1}{uv} + H_{iu}H_{iv} - H_{iu}H_{-1-iv}$$
$$+ H_{-iu}H_{iv} + H_{-1-iu}H_{-iv} - H^{(2)}_{-1+iu} - H^{(2)}_{-1-iv}\Big] + O(g^2)\,, \tag{B.27}$$

$$P_{\mathrm{f}|\mathrm{F}}(u|v) = \frac{i}{u} + \frac{g^2}{u^2}\left[\frac{i}{u} - H_{-1-iv}\right] + O(g^4)\,, \tag{B.28}$$

$$P_{\mathrm{f}|\mathrm{f}}(u|v) = \frac{i}{u-v} - \frac{ig^2}{uv(u-v)} + O(g^4)\,, \tag{B.29}$$

$$P_{\bar{\mathrm{F}}|\mathrm{F}}(u|v) = \frac{\Gamma(1+iu-iv)}{\Gamma(1+iu)\Gamma(1-iv)}$$
$$+ \frac{g^2\Gamma(1+iu-iv)}{\Gamma(1+iu)\Gamma(1-iv)}\Big[H_{iu}H_{-1+iv} - H_{-1+iu}H_{-iv}$$
$$+ H_{-iu}H_{iv} + H_{-iu}H_{-iv} - H^{(2)}_{iu} - H^{(2)}_{-iv}\Big] + O(g^4)\,, \tag{B.30}$$

$$P_{\bar{\mathrm{f}}|\mathrm{F}}(u|v) = 1 + \frac{ig^2}{u}H_{-iv} + O(g^4)\,, \tag{B.31}$$

$$P_{\bar{\mathrm{f}}|\mathrm{f}}(u|v) = 1 + O(g^4)\,. \tag{B.32}$$

The one-loop single-particle and gluon bound state measures are [14,15]

$$\mu_{\mathrm{g}}(u) = -\frac{g^2\pi}{u^+u^-\cosh(\pi u)}$$
$$- \frac{g^4\pi}{2u^+u^-\cosh(\pi u)}\Big[-\big(H_{1/2-iu}+H_{1/2+iu}\big)^2 + 10\zeta_2 - \frac{1-8u^2}{(u^+u^-)^2}$$

$$- \frac{18\zeta_2}{\cosh^2(\pi u)}\Bigg] + O(g^6)\,, \tag{B.33}$$

$$\mu_{\rm h}(u) = \frac{g^2\pi}{\cosh(\pi u)} + \frac{g^4\pi}{\cosh(\pi u)}\Bigg[- H^2_{-1/2-iu} - H^2_{-1/2+iu} + 2\zeta_2\big(1 - 3\mathrm{sech}^2(\pi u)\big)\Bigg] + O(g^6)\,, \tag{B.34}$$

$$\mu_{\rm F}(u) = \frac{g^2\pi}{u\sinh(\pi u)} + \frac{g^4\pi}{u\sinh(\pi u)}\Bigg[- H^2_{-iu} - H^2_{iu} + \frac{1}{u^2} + \frac{\pi\coth(\pi u)}{u} + 2\zeta_2 + \frac{\pi^2}{\sinh^2(\pi u)}\Bigg] + O(g^6)\,, \tag{B.35}$$

$$\mu_{\rm f}(u) = -1 - \frac{g^2}{u^2} + O(g^4)\,, \tag{B.36}$$

$$\mu_{D\rm g}(u) = \frac{g^2\pi u}{(u^2+1)\sinh(\pi u)} + \frac{g^4\pi u}{(u^2+1)\sinh(\pi u)}\Bigg[- H^2_{-iu} - H^2_{iu} - 2\frac{H_{-iu}+H_{iu}}{u^2+1} - \frac{1+6u^2-3u^4}{u^2(u^2+1)^2} + 2\zeta_2 + \frac{\pi^2}{\sinh^2(\pi u)}\Bigg] + O(g^6)\,, \tag{B.37}$$

while the composite two-particle measures of a small fermion accompanying other flux-tube excitations read [16,18]

$$\mu_{\rm fF}(u) = \frac{\pi(u-i)}{\sinh(\pi u)}\Bigg\{g^2 + g^4\Bigg[-H^2_{iu} - H^2_{-iu} + 2\zeta_2 - \frac{1+i\pi\coth(\pi u)}{u(u-i)} + \frac{\pi^2}{\sinh^2(\pi u)}\Bigg] + O(g^6)\Bigg\}\,, \tag{B.38}$$

$$\mu_{\rm hf}(u) = \frac{\pi\left(u-\frac{3i}{2}\right)}{i\cosh(\pi u)}\Bigg\{g^2 + g^4\Bigg[- H^2_{-1/2-iu} - H^2_{-1/2+iu} + 2\zeta_2(1 - 3\,\mathrm{sech}^2(\pi u)) - \frac{\pi\tanh(\pi u)}{u-\frac{3i}{2}}\Bigg] + O(g^6)\Bigg\}\,, \tag{B.39}$$

$$\mu_{\rm gf}(u) = \frac{\pi u^-}{i\cosh(\pi u)}\Bigg\{g^2 + g^4\Bigg[-\tfrac{1}{2}\left(H_{1/2-iu} + H_{1/2+iu}\right)^2 - \frac{\pi\left(3\pi u^- + \sinh(2\pi u)\right)}{2u^-\cosh^2(\pi u)} - \frac{iu}{(u^+u^-)^2} + 5\zeta_2\Bigg] + O(g^6)\Bigg\}\,. \tag{B.40}$$

Finally, we quote the flux-tube dispersion relations to the required order [41,42,12]

$$E_{\rm h} = 1 + 2g^2\left(H_{-1/2-iu} + H_{-1/2+iu}\right) + O(g^4)\,, \qquad p_{\rm h} = 2u - 2g^2\pi\tanh(\pi u) + O(g^4)\,, \tag{B.41}$$

$$E_{\rm g} = 1 + 2g^2\left(H_{1/2-iu} + H_{1/2+iu}\right) + O(g^4)\,, \qquad p_{\rm g} = 2u - 2g^2\pi\tanh(\pi u) + O(g^4)\,, \tag{B.42}$$

$$E_{\rm F} = 1 + 2g^2\left(H_{-iu} + H_{iu}\right) + O(g^4)\,, \qquad p_{\rm F} = 2u - 2g^2\pi\coth(\pi u) + O(g^4)\,, \tag{B.43}$$

$$E_{\rm f} = 1 + O(g^6)\,, \qquad p_{\rm f} = 2g^2/u + O(g^4)\,. \tag{B.44}$$

In the above equations as well as the main body of the paper, we used the definition of the Zhukowski variable

$$x[u] = \tfrac{1}{2}(u + \sqrt{u^2 - (2g)^2})\,, \tag{B.45}$$

as well as the following conventions for shifted rapidities

$$u^{\pm} \equiv u \pm \frac{i}{2}\,, \qquad x^{\pm}[u] \equiv x[u^{\pm}]\,. \tag{B.46}$$

Appendix C. Supplementary material

Supplementary material related to this article can be found online at http://dx.doi.org/10.1016/j.nuclphysb.2015.05.024.

References

[1] N. Beisert, et al., Review of AdS/CFT integrability: an overview, Lett. Math. Phys. 99 (2012) 3, arXiv:1012.3982 [hep-th].
[2] L.F. Alday, D. Gaiotto, J. Maldacena, A. Sever, P. Vieira, An operator product expansion for polygonal null Wilson loops, J. High Energy Phys. 1104 (2011) 088, arXiv:1006.2788 [hep-th].
[3] B. Basso, A. Sever, P. Vieira, Spacetime and flux tube S-matrices at finite coupling for $N = 4$ supersymmetric Yang–Mills theory, Phys. Rev. Lett. 111 (9) (2013) 091602, arXiv:1303.1396 [hep-th].
[4] L.F. Alday, J.M. Maldacena, Gluon scattering amplitudes at strong coupling, J. High Energy Phys. 0706 (2007) 064, arXiv:0705.0303 [hep-th].
[5] J.M. Drummond, J. Henn, G.P. Korchemsky, E. Sokatchev, On planar gluon amplitudes/Wilson loops duality, Nucl. Phys. B 795 (2008) 52, arXiv:0709.2368 [hep-th].
[6] A. Brandhuber, P. Heslop, G. Travaglini, MHV amplitudes in $N = 4$ super Yang–Mills and Wilson loops, Nucl. Phys. B 794 (2008) 231, arXiv:0707.1153 [hep-th].
[7] S. Caron-Huot, Notes on the scattering amplitude/Wilson loop duality, J. High Energy Phys. 1107 (2011) 058, arXiv:1010.1167 [hep-th].
[8] L.J. Mason, D. Skinner, The complete planar S-matrix of $N = 4$ SYM as a Wilson loop in Twistor space, J. High Energy Phys. 1012 (2010) 018, arXiv:1009.2225 [hep-th].
[9] A.V. Belitsky, G.P. Korchemsky, E. Sokatchev, Are scattering amplitudes dual to super Wilson loops?, Nucl. Phys. B 855 (2012) 333, arXiv:1103.3008 [hep-th].
[10] J.M. Drummond, J. Henn, G.P. Korchemsky, E. Sokatchev, Dual superconformal symmetry of scattering amplitudes in $N = 4$ super-Yang–Mills theory, Nucl. Phys. B 828 (2010) 317, arXiv:0807.1095 [hep-th].
[11] L.J. Mason, D. Skinner, Dual superconformal invariance, momentum twistors and grassmannians, J. High Energy Phys. 0911 (2009) 045, arXiv:0909.0250 [hep-th].
[12] B. Basso, Exciting the GKP string at any coupling, Nucl. Phys. B 857 (2012) 254, arXiv:1010.5237 [hep-th].
[13] B. Basso, A.V. Belitsky, Lüscher formula for GKP string, Nucl. Phys. B 860 (2012) 1, arXiv:1108.0999 [hep-th].

[14] B. Basso, A. Sever, P. Vieira, Space–time S-matrix and flux tube S-matrix II. Extracting and matching data, J. High Energy Phys. 1401 (2014) 008, arXiv:1306.2058 [hep-th].
[15] B. Basso, A. Sever, P. Vieira, Space–time S-matrix and flux-tube S-matrix III. The two-particle contributions, J. High Energy Phys. 1408 (2014) 085, arXiv:1402.3307 [hep-th].
[16] A.V. Belitsky, Nonsinglet pentagons and NHMV amplitudes, arXiv:1407.2853 [hep-th].
[17] B. Basso, A. Sever, P. Vieira, Space–time S-matrix and flux-tube S-matrix IV. Gluons and fusion, J. High Energy Phys. 1409 (2014) 149, arXiv:1407.1736 [hep-th].
[18] A.V. Belitsky, Fermionic pentagons and NMHV hexagon, arXiv:1410.2534 [hep-th].
[19] B. Basso, J. Caetano, L. Cordova, A. Sever, P. Vieira, OPE for all helicity amplitudes, arXiv:1412.1132 [hep-th].
[20] V. Del Duca, C. Duhr, V.A. Smirnov, The two-loop hexagon Wilson loop in $N = 4$ SYM, J. High Energy Phys. 1005 (2010) 084, arXiv:1003.1702 [hep-th].
[21] A.B. Goncharov, M. Spradlin, C. Vergu, A. Volovich, Classical polylogarithms for amplitudes and Wilson loops, Phys. Rev. Lett. 105 (2010) 151605, arXiv:1006.5703 [hep-th].
[22] L.J. Dixon, J.M. Drummond, M. von Hippel, J. Pennington, Hexagon functions and the three-loop remainder function, J. High Energy Phys. 1312 (2013) 049, arXiv:1308.2276 [hep-th].
[23] L.J. Dixon, J.M. Drummond, C. Duhr, J. Pennington, The four-loop remainder function and multi-Regge behavior at NNLLA in planar $N = 4$ super-Yang–Mills theory, J. High Energy Phys. 1406 (2014) 116, arXiv:1402.3300 [hep-th].
[24] L.J. Dixon, J.M. Drummond, J.M. Henn, Analytic result for the two-loop six-point NMHV amplitude in $N = 4$ super Yang–Mills theory, J. High Energy Phys. 1201 (2012) 024, arXiv:1111.1704 [hep-th].
[25] L.J. Dixon, M. von Hippel, Bootstrapping an NMHV amplitude through three loops, arXiv:1408.1505 [hep-th].
[26] J. Golden, M.F. Paulos, M. Spradlin, A. Volovich, Cluster polylogarithms for scattering amplitudes, arXiv:1401.6446 [hep-th].
[27] J. Golden, M. Spradlin, An analytic result for the two-loop seven-point MHV amplitude in $\mathcal{N} = 4$ SYM, J. High Energy Phys. 1408 (2014) 154, arXiv:1406.2055 [hep-th].
[28] J. Golden, M. Spradlin, A cluster bootstrap for two-loop MHV amplitudes, arXiv:1411.3289 [hep-th].
[29] J.M. Drummond, G. Papathanasiou, M. Spradlin, A symbol of uniqueness: the cluster bootstrap for the 3-loop MHV heptagon, arXiv:1412.3763 [hep-th].
[30] B. Basso, J. Caetano, L. Cordova, A. Sever, P. Vieira, in preparation.
[31] A.V. Belitsky, S.E. Derkachov, A.N. Manashov, Quantum mechanics of null polygonal Wilson loops, Nucl. Phys. B 882 (2014) 303, arXiv:1401.7307 [hep-th].
[32] A.V. Belitsky, OPE for null Wilson loops and open spin chains, Phys. Lett. B 709 (2012) 280, arXiv:1110.1063 [hep-th].
[33] A. Sever, P. Vieira, T. Wang, From polygon Wilson loops to spin chains and back, J. High Energy Phys. 1212 (2012) 065, arXiv:1208.0841 [hep-th].
[34] S. Caron-Huot, S. He, Jumpstarting the all-loop S-matrix of planar $N = 4$ super Yang–Mills, J. High Energy Phys. 1207 (2012) 174, arXiv:1112.1060 [hep-th].
[35] J.L. Bourjaily, S. Caron-Huot, J. Trnka, Dual-conformal regularization of infrared loop divergences and the chiral box expansion, arXiv:1303.4734 [hep-th].
[36] D. Gaiotto, J. Maldacena, A. Sever, P. Vieira, Pulling the straps of polygons, J. High Energy Phys. 1112 (2011) 011, arXiv:1102.0062 [hep-th].
[37] G. Papathanasiou, Hexagon Wilson loop OPE and harmonic polylogarithms, J. High Energy Phys. 1311 (2013) 150, arXiv:1310.5735 [hep-th].
[38] Y. Hatsuda, Wilson loop OPE, analytic continuation and multi-Regge limit, J. High Energy Phys. 1410 (2014) 38, arXiv:1404.6506 [hep-th].
[39] A. Sever, P. Vieira, Multichannel conformal blocks for polygon Wilson loops, J. High Energy Phys. 1201 (2012) 070, arXiv:1105.5748 [hep-th].
[40] L.F. Alday, J.M. Maldacena, Comments on operators with large spin, J. High Energy Phys. 0711 (2007) 019, arXiv:0708.0672 [hep-th].
[41] A.V. Belitsky, A.S. Gorsky, G.P. Korchemsky, Logarithmic scaling in gauge/string correspondence, Nucl. Phys. B 748 (2006) 24, arXiv:hep-th/0601112.
[42] A.V. Belitsky, G.P. Korchemsky, R.S. Pasechnik, Fine structure of anomalous dimensions in $N = 4$ super Yang–Mills theory, Nucl. Phys. B 809 (2009) 244, arXiv:0806.3657 [hep-ph].